N75-13865

NASA TECHNICAL MEMORANDUM

NASA TM X- 71972

COPY NO.

NASA TM X- 71972

(NASA-TM-X-71972) SCRAMJET NOZZLE DESIGN AND ANALYSIS AS APPLIED TO A HIGHLY INTEGRATED HYPERSONIC RESEARCH AIRPLANE (NASA) 56 p HC $4.25 CSCL 21E

N75-13865

Unclas
G3/07 05043

SCRAMJET NOZZLE DESIGN AND ANALYSIS AS APPLIED TO A HIGHLY INTEGRATED HYPERSONIC RESEARCH AIRPLANE

BY WILLIAM J. SMALL, JOHN P. WEIDNER, AND P. J. JOHNSTON

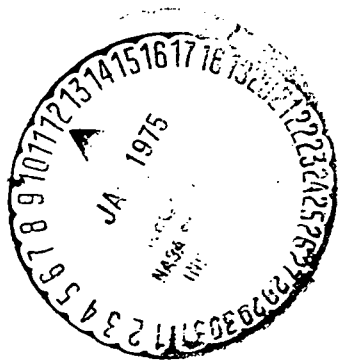

NOV. 1974

NATIONAL AERONAUTICS AND SPACE ADMINISTRATION
LANGLEY RESEARCH CENTER, HAMPTON, VIRGINIA 23665

SCRAMJET NOZZLE DESIGN AND ANALYSIS AS APPLIED TO A HIGHLY INTEGRATED HYPERSONIC RESEARCH AIRPLANE

by William J. Small, John P. Weidner, and P. J. Johnston

SUMMARY

The great potential expected from future airbreathing hypersonic aircraft systems is predicated on the assumption that the propulsion system can be efficiently integrated with the airframe. A study of engine-nozzle airframe integration at hypersonic speeds has been conducted using a high speed research aircraft concept as a focus. Recently developed techniques for analysis of scramjet nozzle exhaust flows provide a realistic analysis of complex forces resulting from the engine-nozzle airframe coupling. Results from these studies show that by properly integrating the engine-nozzle propulsive system with the airframe, efficient controlled and stable flight will result over a wide speed range.

INTRODUCTION

Studies of hypersonic airbreathing aircraft using hydrogen fuel have shown them to have unique and desirable characteristics as future flight systems (ref. 1, 2, 3, 4, 5). The high speeds typical of these vehicles make them attractive for a variety of missions such as long range civil transports, launch vehicles for second stage orbiters and a variety of military applications. The expected flight regimes of these aircraft are illustrated in figure 1. Efficient airbreathing propulsion systems utilizing ramjet-scramjet engine cycles are critical developmental items and constitute a pacing item in hypersonic aircraft development. The propulsion system installation for very high speed flight will differ from conventional concepts in that a higher degree of commonality is required between airframe and engine components.

As illustrated in figure 2, the entire vehicle undersurface is devoted to the propulsion system. The forebody acts as an inlet compression ramp, a center portion of the body contains engine modules, and the complete afterbody forms an exhaust nozzle surface.

Previous studies (refs. 6, 7, 8) have found these integrated concepts to have beneficial aspects for both cruise and acceleration applications. Advantages that accrue from efficient engine-airframe integration include forebody inlet precompression which effectively reduces required engine size and weight requirements as compared to a free stream inlet and because some of the work of inlet compression has been accomplished by this forebody, overall engine efficiency is improved. Exhaust nozzle performance also benefits from this integrated concept since the large afterbody nozzle area can potentially provide very efficient exhaust gas expansion with minimal aerodynamic drag. This

large exhaust surface can also be used advantageously to increase favorable lift for cruise aircraft.

Integration of engine and airframe in this highly integrated manner, however, is not the only solution to the design of hypersonic propulsion systems. An alternate concept incorporates axisymmetric engines and nozzles contained within discrete nacelles in a manner similar to current podded turbojet engines. The study of reference 9, specifically addresses these alternate concepts and concludes that integrated systems such as will be studied in this paper offer a much higher installed specific impulse as compared to axisymmetric systems.

It is apparent that the large exhaust surfaces of highly coupled, integrated aircraft can produce large thrust and moment forces and, in the case of an improperly designed nozzle, associated trim drag penalties may become excessive. Since nozzle design is primarily controlled by thrust and stability requirements, it is imperative that propulsion system parameters be examined across the entire aircraft flight envelope. Vehicle trim capability in the power-off mode also assumes increased importance due to the possible large shift in thrust vectors and resulting trim requirements. Therefore, one key to a successful high performance vehicle is a systematic procedure for effectively assessing these interactions in the early stages of a design if any beneficial coupling between the engine, nozzle and airframe is to be achieved.

A study of the interactions between propulsion and aerodynamics of a highly integrated vehicle was undertaken in support of a Langley Research Center research airplane conceptual design effort and is partially described in references 10 and 11. Its mission was to act as a test vehicle for key hypersonic technology items such as structural and thermal protection system concepts, and propulsion package operation under true flight conditions

throughout most of the hypersonic flight regime of interest (fig. 1). Propulsion system concepts and trends developed during the course of this study, because of the highly integrated nature of this vehicle and the large range of flight conditions that had to be evaluated, should apply to a large class of hypersonic vehicles. The results, concepts and techniques developed for engine-nozzle-airframe integration as a result of this study, form the subject of this paper.

The organization of the paper is summarized below:

I. GENERAL STUDY CONSIDERATIONS: Background material is presented for the research vehicle and scramjet engine module of this study. Fundamental engine sizing constraints are also discussed.

II. ANALYTICAL TECHNIQUES: Ground rules for this study and analytical methods for computing airframe and propulsion system components are summarized. Engine-airframe force data bookkeeping procedures are outlined.

III. PARAMETRIC STUDY OF NOZZLE: Nozzle geometry and longitudinal engine-nozzle locations are parametrically varied to determine their effect on nozzle operation and the resulting integrated trimmed vehicle performance.

IV. VEHICLE PERFORMANCE - PROPULSION: A candidate nozzle determined to be near optimum from the previous parametric study is used to investigate vehicle stability and acceleration performance.

SYMBOL LIST

A	Area
A_1	Inlet capture Area
A_4	Ideal one-dimensional exhaust area
A_I	Inlet area
C_L	Lift coefficient $(\frac{\text{lift}}{q_\infty S_{ref}})$
C_M	Pitching moment coefficient $(\frac{\text{pitching moment}}{\text{vehicle length}})/q_\infty S_{ref}$
C_S	Spillage force coefficient
C_T	Thrust coefficient in the flight direction $(\frac{T}{q_\infty S_{ref}})$
C_{T_E}	Engine thrust coefficient in plane of engine $(\frac{\text{engine thrust}}{q_\infty S_{ref}})$
C_{T_S}	Cowl thrust coefficient $(\frac{\text{cowl force}}{q_\infty S_{ref}})$
C_{T_W}	Nozzle wall thrust coefficient $(\frac{\text{wall force}}{q_\infty S_{ref}})$
C_σ	Isolated nozzle thrust coefficient
D	Drag
E	Combustor exit height
F_X	Axial inlet spillage force
F_Y	Normal inlet spillage force
H	Inlet height
H_2	Hydrogen
ISP	Specific Impulse
L	Length
L/D	Lift to drag ratio
M	Mach number

P	Pressure
q	Dynamic pressure
S_{ref}	Vehicle reference area
T	Thrust, temperature °K
V	Velocity, n/m^2
V_s	Satellite velocity
α	Angle of attack, incidence, deg
δ_e	Elevon deflection angle (positive when trailing edge is down)
θ	Surface incidence
σ	Angle between engine-nozzle axis and flight direction
ϕ	Equivalence ratio (percent of stoichiometric fuel to air ratio)

Subscripts

1	Airflow properties prior to inlet entrance
3	Combustor exit conditions
∞	Free stream
AC	Aerodynamic center
C	Combustor exit
E	Engine
F	Forebody
I	Inlet
M	Moment
N	Nozzle
S	Cowl
V	Vehicle
W	Wall
X	Axial direction
Y	Normal direction

GENERAL STUDY CONSIDERATIONS

A Langley Research Center design study of conceptual high speed research airplanes, investigated a series of alternate candidate concepts. From these concepts a highly integrated hydrogen fueled design was selected as the focus for this propulsion integration study, since it incorporated many of the significant features of future hypersonic aircraft such as large afterbody areas for nozzle expansion. This vehicle and its associated scramjet propulsion package are next summarily described.

Hydrogen fueled hypersonic research aircraft.- The hypersonic research aircraft used as the basis for the engine-nozzle-vehicle integration analysis described in this paper (figures 2,3), is 24.4m long and is powered by four RL-10 rocket engines fueled with liquid hydrogen and liquid oxygen. Sufficient propellant is contained within the aircraft for rocket acceleration to Mach 8 from an air launch at Mach 0.8, with additional propellant for Mach 10 boost provided by external tanks that would jettison at about Mach 2. As illustrated in figures 2 and 3, six research scramjet modules can be integrated with the basic aircraft. With efficient integration the scramjets can provide accelerating thrust between Mach 4 and 10 without rocket power.

LRC fixed geometry scramjet.- The baseline research scramjet employed in this study is the fixed geometry concept currently under development at Langley Research Center (ref. 9, 10, 12, 13). This is a rectangular modular engine that attaches directly to the vehicle undersurface. This concept uses swept compression surfaces and fuel injector struts to provide inlet starting at low speed and good internal performance throughout the scramjet operating speed range. The swept compression surfaces also provide localized pressure relief

along the top surface of the engine to enable the scramjet to ingest the vehicle forebody boundary layer, thus eliminating the need for boundary layer diversion or bleed. In-stream fuel injection is used to minimize the combustor length and heat flux to the internal surfaces. The engine operates in a supersonic combustion mode at speeds above Mach 5. Calculations show thermal choking within the combustor may occur below Mach 5 if supersonic combustion were attempted and may result in a mode of operation involving both subsonic and supersonic combustion.

Engine size constraints.- A primary objective of the conceptual research airplane study was to define an integrated vehicle airbreathing propulsion system capable of demonstrating acceleration and high component performance throughout a wide hypersonic speed range. Mission analysis studies indicated that good aircraft acceleration throughout the scramjet operating range was of paramount importance. Accordingly, the engine inlet was always sized to take full advantage of the maximum useable area within the forebody shock layer. Inlets designed to extend through the shock layer into free stream flow are considered unlikely possibilities from the standpoint of reduced engine performance and increased weight requirements, and were not considered. Increased Mach number generally requires an increasing engine size as a result of reduced air density and specific impulse. At the same time increased Mach number decreases the depth of the forebody lower surface shock layer such that the inlet must be located at a more rearward body station where sufficient airflow is available. The vehicle forebody has a major influence on the size engine that can be installed at any given body station through minimizing flow angularity and maximizing available mass flow available for processing at the inlet face. A good forebody design allows a maximum utilization of the available area

within the body shock layer. Details of the forebody design and analysis is the subject of reference 10.

While the effect of higher Mach numbers is to move the engine location rearward to maximize engine size, at the same time the larger nozzle expansion areas needed to maximize thrust at higher Mach numbers have the effect of increasing nozzle length and forcing the engine forward. Figure 4 illustrates the ideal expansion area required for fully expanded nozzles for the case of isentropically expanding hydrogen-air combustion products. The isentropic conditions shown represent uniform parallel entrance and exit nozzle flows expanding to a single specified exit pressure. Practically, however, such a nozzle is too long for most hypersonic aircraft applications, and true nozzle exit conditions are far from uniform. This nonuniformity results from the fact that the nozzle upper wall has the capability to expand to near stream pressure before overexpanding, yet the nozzle interior cowl wall pressure can only expand to the higher external cowl pressure before it overexpands. Nonetheless, the manner in which ideal exhaust expansion area requirements tend to increase with Mach number is,in general,indicative of the trend of practical nozzles.

ANALYTICAL TECHNIQUES

A complete analysis of the impact of propulsion system variables on total aircraft performance involves a large spectrum of flight conditions for each propulsion system variable considered. The preliminary analysis reported herein, however, confined the engine-nozzle-airframe design study to a 71,850 n/m^2 (1500 psf) acceleration flight path from Mach 4 (scramjet ignition) to Mach 10 (maximum aircraft Mach number). The engine-nozzle-airframe combination was analyzed at an aircraft angle-of-attack of two degrees, which was

representative of the 71,850 n/m^2 flight path, and total trimmed aircraft thrust margin was the primary criteria of merit for evaluating the engine nozzle combinations. The propulsion system was analyzed at the discrete Mach numbers of 4, 6, and 10, and the following Mach number/fuel-air ratio schedule was determined to be near optimum from missions studied:

Mach No.	Ø
4.0	1.0
6.0	1.0
10.0	1.5

Several analytical methods were required to compute the major airframe, engine, and nozzle forces and the essential elements of these techniques are summarized as follows:

Airframe analysis.- Aerodynamics of the basic vehicle and external engine cowl surfaces were evaluated using the hypersonic arbitrary body program of reference 14 by selecting the following program options. Body and cowl compression surface pressures were computed using tangent cone methods, and compression surface pressures on wings, tails, and control surfaces were computed using tangent wedge methods. All pressure on aerodynamic surfaces in expansion was determined by Prandtl-Meyer expansion from free stream. Turbulent skin friction was calculated by the method of Spalding and Chi.

Engine Analysis.- Engine module performance was analyzed using one-dimensional techniques for either a pure scramjet cycle (references 9 and 13) or pure ramjet cycle (reference 15). Scramjet (supersonic combustion) engine performance was calculated at discrete Mach numbers of 4, 6, and 10, and ramjet (subsonic combustion) engine module performance was calculated at Mach 4. Mission

analysis studies for this vehicle indicated that fuel-to-air ratios near stoichiometric were required to produce acceptable acceleration performance at Mach 4. A fuel-to-air ratio near stoichiometric could not be obtained in a pure scramjet cycle at this low Mach number because of thermal choking. Therefore, for the purposes of this study, ramjet engine performance was used at Mach 4 and scramjet engine performance was used at Mach 6 and 10. These calculations were used not only to assess internal engine performance, but also to provide the initial conditions for the nozzle calculations. Inlet entrance and combustor exit conditions are presented in table 1.

Nozzle analysis.- Six discrete scramjet modules were combined to form the complete engine system for the aircraft as shown in figures 2 and 3. Uniform two-dimensional flow exhausting from a single combustor exit was assumed to represent the engine package; thus, for purposes of this study the assumption was made that combustor exit geometry, instead of forming a series of six discrete rectangular combustor exits exhibiting three-dimensional flow, would be modified to a single rectangular two-dimensional exit spanning the entire width of the engine package. In order to preserve exit area with this greater width, the two-dimensional combustor exit height was reduced from the three-dimensional case. In all cases presented in this paper the resulting two-dimensional ratio of combustor exit height to engine inlet height is held constant.

Nozzle forces were analyzed using a recently developed three-dimensional reference plane characteristics computer program in a two-dimensional mode of operation (ref. 16). As stated earlier, engine cycle calculations were used to obtain initial conditions and thereafter exhaust gas properties were internally generated by the nozzle program for proper hydrogen-air combustion product mixtures in local chemical equilibrium. The interaction between nozzle

flow and external flow was computed for all cases of nozzle underexpansion. Nozzle geometry was assumed strictly two dimensional from the combustor exit plane rearward (figure 5). Nozzle wall contours were linear segments joined by small radii to insure surface slope continuity. Note that combustor exit conditions are assumed to begin in a vertical rather than the sweptback plane typical of this engine concept. It is realized that three-dimensional effects are of importance in nozzle design; however, in this preliminary effort emphasis was placed on major trends in nozzle design that could be discerned without the additional complexity of three dimensionality. Subsequent analysis should investigate three-dimensional effects to the limit of available theoretical and experimental methods.

External cowl surfaces.- Sidewall surfaces of the engine cowling were approximately aligned with the flow under the body. The cowling lower surface, on the other hand, is inclined into the flow with an angle determined by the nozzle cowl wall geometry (figure 5). Changes in this nozzle cowl wall geometry thus necessarily involves changes in exterior cowl aerodynamic forces which were accounted for in all integrated vehicle calculations. As a result of the forebody analysis of reference 10, the engine inlet cowling was designed to subtend approximately 80 percent of the body lower surface width as shown in figure 3. For this vehicle, this is the maximum engine width commensurate with reasonably uniform flow within the forebody shock layer flow.

Engine spillage.- Engine spillage is a design feature of this fixed geometry engine that allows operation at low Mach numbers. The spillage schedule was taken from reference 13 (figure 6a) and was used in computing engine performance. Spillage forces are caused by the deflection of spillage air by the engine inlet external shock system and are presented in figure 6b. These

values were computed through a theoretical evaluation of integrated forces along the engine spillage streamtube. It was assumed that engine spillage did not affect engine cowl pressures.

Definition of forces.- For purposes of analysis and presentation of data, the propulsion system forces were subdivided into several categories which were separately calculated and then used in the total vehicle force integrations. One of these categories, the engine module forces, contain all interior forces of the propulsion system from the beginning of the module inlet through the combustor. The component of engine thrust in the flight direction is denoted as net engine module thrust. Note that the engine module will develop net lift and pitching moments which are accounted for in total integrated vehicle force summations.

The second general category of propulsion system forces, the nozzle forces, include all surface forces (upper nozzle wall and interior cowl wall) extending rearward from the combustor exit. Nozzle force summations do not include net engine module forces nor external cowl forces. Nozzle thrust coefficients presented in this paper are calculated in the flight axis direction unless otherwise noted and the nozzle moments are taken about the vehicle center-of-gravity (64.5 percent of body length). This C.G. location is held constant throughout the study for all nozzle and engine locations. Nozzle lengths are nondimensionalized by combustor exit height since this length-to-height ratio characterizes those portions of the nozzle geometry affected by expansion fans emanating from either the nozzle wall or cowl surfaces. Nozzle forces and moments used in this study are presented in table 2.

The last category of propulsion system forces, external forces, includes spillage and external cowl aerodynamic forces which are accounted for in all force summations.

Aerodynamic forces are computed over the entire vehicle surface not subtended by the propulsion system components (inlet, exterior cowling, and nozzle). Note that the forces on the vehicle forebody ahead of the inlet entrance are not included as part of the propulsion system, but rather as an integral part of the airframe aerodynamics.

PARAMETRIC STUDY OF NOZZLE

The purpose of the nozzle optimization analysis was to assess the effects of nozzle geometry modifications (figure 5) on aircraft performance (primarily thrust margin and trim control) and to determine optimum combinations of the nozzle variables for the research airplane configuration. The longitudinal location of the scramjet, upper nozzle wall angle, interior cowl angle, and cowl length measured from the combustor exit were the primary independent nozzle variables used to optimize the engine nozzle combination and its effect on vehicle performance. Note that the lower cowl exterior surface angle was determined by the interior cowl angle (θS) and cowl length (L_S).

In principle, global optimums for these variables could be found using a parameter minimization technique. Such a procedure was impractical for this study because of the mass of data processing required to establish a single variation from a given reference point. Instead variations in nozzle geometry were made from a baseline nozzle selected early in the study on the basis of good performance characteristics at Mach 10 as described later in the Scramjet Location section. The use of this baseline nozzle offers a convenient

reference to gauge the relative merits of the parametric nozzle variations presented. The baseline nozzle upper wall was characterized by a 20 degree upper wall expansion angle and a length 18.54 times combustor height. The nozzle lower cowl opened at a six degree expansion angle and was 3.12 times as long as the combustor exit height. The geometric proportions of this nozzle are depicted in the sketch on figure 5.

Scramjet location.- Early in the study, scramjet engine longitudinal location on the aircraft at Mach 10 was found to be one of the most crucial variables to be determined. At this high speed end of the flight trajectory, engine thrust margins decline due to reduced engine performance. In addition, vehicle control requirements can be very severe due to reduced static margins at these high Mach numbers. Any large control deflections at Mach 10 imply large elevon drag and heating loads.

The method used in sizing the propulsion system package as axial location changed (figure 7) was to increase engine inlet area as the engine was moved rearward in order to capture the maximum available shock layer flow. This sizing was accomplished by assuming a constant engine width of approximately 80 percent of body span and a linear variation in shock height with longitudinal position. These assumptions were shown to be reasonable from the forebody design study of reference 10. The nozzle was held to a maximum geometric expansion area by always terminating the nozzle upper wall just below the aft mounted rocket engine (figure 3). Under these constraints the axial location of the engine determines the nozzle upper wall expansion angle.

The optimum longitudinal engine module-nozzle position depends on inlet mass flow rates, nozzle efficiency and trim drag penalties induced by the propulsion system. Rearward propulsion system location will increase inlet area

and,consequently,mass flow rates through the engine modules,and directly increases engine module thrust. Nozzle thrust, on the other hand, is not a simple function of mass flow rates because, as the engine is moved longitudinally, nozzle geometry and,consequently,efficiency,vary. Trim drag penalties can be induced by both engine location and nozzle configuration. Nozzle efficiency, or the ability to convert nozzle entrance momentum into useful thrust,is primarily a complex function of nozzle geometry. In order to clarify the influence of this nozzle geometry on thrust efficiency, isolated nozzles with constant nozzle entrance conditions typical of a scramjet engine operating with eight degrees of forebody precompression will first be examined. Cowl lengths and the nozzle exit-to-entrance area ratio are also held constant. Thus, the only variables are upper wall expansion angle and length. The geometrical variations in these isolated nozzles are seen from the upper portion of figure 8 to be quite similar to the variations encountered in positioning a nozzle in various longitudinal locations as shown in figure 9, but unlike the true flight case these isolated nozzles are free from variations in mass flow and nozzle exit-to-inlet area variations.

Typically, axisymmetric rocket or turbojet engine nozzles have a clearly defined nozzle exit and the thrust vector lies in the plane of the nozzle axis. The highly integrated scramjet nozzle, on the other hand, as shown in the force diagram of figure 8, may have very large asymmetric components normal to the conventional nozzle axis (defined as parallel to the nozzle entrance flow). Note that as a result of wall radii and angularity, nozzle force vectors do not lie normal to their associated wall inclination angles. If nozzle efficiency is evaluated on the basis of thrust generated along the

nozzle axis, the smallest expansion angle (longest nozzle) develops the largest thrust. This is to be expected (assuming inviscid flow) since small upper wall angles will reduce the strength of the upper wall expansion fan and thus increase nozzle upper wall pressures. However, the thrust in the flight direction determines vehicle acceleration characteristics and the flight axis of the research aircraft used in this study is inclined eight degrees to the nozzle axis. Since nozzle thrust levels in the flight direction depend upon both the magnitude and orientation of the forces generated on the nozzle upper wall, the optimum nozzle for producing thrust in the flight direction is not the lowest expansion angle (longest) nozzle but is shorter and has a greater upper wall expansion angle as indicated in figure 8.

For a condition of constant mass flow and in the absence of trim drag, the 20 degree nozzle would be selected as an optimum from an installed thrust standpoint. The true situation in regard to longitudinally placing the engine-nozzle, however, is complicated by the fact that as the engine is moved rearward from the most efficient nozzle position, the nozzle assumes a less efficient shape, inlet mass flow increases, and aircraft trim requirements change. This situation can be best explained by reference to figures 9 and 10 which schematically and graphically illustrate engine-nozzle behavior with axial location. As the nozzle is shifted rearward net engine module and cowl forces increase in direct proportion to ingested mass flow. Upper wall forces, however, decrease as the nozzle shifts rearward and also incline more into the direction of the flight axis. The net result of engine module plus nozzle forces is seen (fig. 10) to increase in net thrust levels as the nozzle is moved rearward to the 70 percent body station with only small increases past that point. Thus, increased mass flow at the rearmost engine-nozzle axial locations was more than able to

compensate for the poor efficiency of the large wall angle nozzles. Trim drag penalties on the integrated airplane are a function of nozzle thrust and lift induced pitching moments and can strongly influence the selection of an optimum nozzle. The magnitude of wall and cowl forces presented in figures 9 and 10 show that for the engine module located at 0.694 of body length nozzle moments are nearly canceled by net engine module moments. As the engine is moved aft of this location, large positive moments are introduced as a result of the reduced nozzle upper wall and increased cowl pressures, a condition which is aggravated by an increasing moment arm to the vehicle center of gravity. In actual practice the aircraft center of gravity may move somewhat rearward with aft movement of the engine and associated changes in vehicle internal packaging and structural arrangements. Such a C. G. travel may be limited, however, since it aggravates an already marginal stability problem at the highest Mach numbers (see Longitudinal Stability). Refined treatment of the propulsion integration problem must of course include realistic C. G. travel in the design trades.

The net effect of scramjet location on thrust margin and elevon deflections required for trim is shown in figure 11 for the research airplane. As previously shown the decrease in nozzle efficiency with the more rearward engine locations tends to counterbalance the beneficial effects of increased mass flow such that only slight increases in untrimmed thrust margins are obtained for engine locations aft of $L_E/L_V = 0.7$. However, the large positive pitching moments associated with the rearward engine location require large positive elevon trim control. As shown, trim drag associated with these positive elevon deflections prevents the most rearward nozzle from producing a maximum integrated thrust margin, despite the larger inlet capture area associated with this location. Elevon deflections are essentially zero and the thrust margin

is a maximum at an engine position 0.05 L_V aft of the center of gravity ($L_E/L_V = 0.7$). Here nozzle forces approximately cancel engine module moments and the aircraft is nearly self trimming. At the more forward engine positions the net negative pitching moments generated by the propulsion system are canceled out by negative elevon deflections which cause a negligible drag penalty for this two degree angle-of-attack case. Thrust margins, however, decrease for these longer nozzles due to large asymmetrical nozzle forces developed along the nozzle upper wall surface. For example, as shown in figure 9, the more forward nozzles (smaller wall angles) develop the largest upper wall forces, but actually produce less thrust in the flight direction than the more rearward nozzles (larger wall angles).

Mission studies have shown that the two degree angle of attack assumed closely approximates a constant 71,850 n/m^2 (1500 psf) trajectory for this aircraft; however, nozzles with large elevon trim changes can be expected to deviate somewhat from this angle of attack to maintain correct lift at a constant dynamic pressure. However, moderate changes in angle-of-attack would not alter the basic comparisons shown in figure 11, as will be shown in a later section of this paper (Acceleration Performance).

Parametric cowl length variations will be reviewed in a later section of this paper but at this point a brief discussion of cowl length effects on nozzles at various longitudinal locations seems in order. Lift forces generated on upper nozzle walls and the lower cowl are each approximately three times the nozzle thrust level and it might be suspected that variations in cowl length would provide a powerful means of controlling trim drag penalties, and thus greatly influence the thrust margins presented in figure 11. In particular, a reduction in cowl length for the most rearward nozzle ($L_E/L_V = 0.775$)

should reduce trim drag and thereby increase the effectiveness of this nozzle. However, as indicated on figure 12, variations in cowl length at this rearward location has little or no effect on total vehicle thrust margins because decreases in trim drag are counterbalanced by thrust losses due to shortening the cowl. At the more forward scramjet positions, shortening the cowl significantly reduces overall nozzle thrust levels. Increases in cowl length at forward scramjet locations beyond that of the baseline nozzle ($L_S/E = 3.0$) tend to result in only slight improvements in thrust margin. Thus, optimum scramjet location is nearly independent of cowl length and occurs at approximately 70 percent of the length for the research vehicle concept.

Propulsion system analysis - baseline nozzle.- From the preceding discussion of engine-nozzle axial location at Mach 10, an optimum location was found at 0.694 of body length. The nozzle corresponding to this location was selected as the baseline nozzle for parametric variations that follow in this paper. At this point, however, a brief analysis of propulsion system forces and efficiencies for this baseline nozzle will be presented over the operational Mach number range.

Computed integrated vehicle forces and moments are presented in figure 13, for Mach numbers 4 through 10. Primary propulsion system forces and moments are predominantly due to nozzle and engine components. Nozzle thrust is seen to play an increasingly critical role as the Mach number increases, and above Mach 6 nozzle thrust exceeds net engine module thrust. Spillage and cowl forces produce net drag, but are relatively insignificant compared to nozzle and engine module thrust and will not be again presented in force breakdowns in this paper, although they have been accounted for in all integrated vehicle force and moment calculations.

Propulsion system specific impulse ratioed to the Mach 10 value is presented for the baseline nozzle in figure 14. This impulse includes net propulsion system forces in the flight direction from the engine-module inlet face to the nozzle exit with all pressures involved in the thrust calculation referenced to free-stream conditions. Results shown in the figure are very similar to those presented in references 9 and 13 which were derived from more idealized considerations.

Nozzle expansion area.- In this section, nozzle geometric expansion area is varied by changing nozzle upper wall angle, θ_w, at constant scramjet location (0.7 L_V), in contrast to a previous section (Scramjet Location) where wall angle was varied and geometric expansion area remained constant. The nozzle sketch shown in figure 15a illustrates this geometric variation. An inspection of the nozzle wall pressure distribution (M = 10) reveals that, as could be expected, increasing wall expansion angle decreases upper wall pressures. Cowl pressures remain constant since the cowl trailing edge terminates forward of any final expansion wave emanating from the upper wall/combustor exit juncture. Typically, those nozzles with small upper surface expansion angles generate large negative pitching moments due to the substantial lift forces involved across the operational Mach number range of the engine.

The largest expansion area nozzle that could be installed in the research airplane (19.8° developed the smallest negative moment and generally counterbalanced net engine moments (fig. 15b)). This large expansion nozzle also consistently developed the largest thrust over the speed range. Figure 16 shows the effect of integrating these nozzles with the total vehicle. The largest nozzle opening that could be fitted to the vehicle (19.8° reference nozzle) is superior to any smaller nozzle opening angle at all Mach numbers,

and undoubtably a somewhat larger opening angle would improve vehicle performance to some extent at the high Mach number end of the flight regime.

The 19.8° nozzle also produces minimum trim drag (figure 16). This nozzle requires only a six degree elevon setting variation from Mach 4 to 10 and requires the least elevon change to transition from trimmed power-on to trimmed power-off flight conditions. The effects of a fuel shutdown (power off conditions) are characterized by engine module drag instead of thrust and decreased nozzle upper and lower wall pressures which for the 19.8° nozzle nearly compensate one another.

Nozzle cowl angle.- A portion of the analysis was devoted to an examination of the effect of interior cowl angle variations (figure 17). Because of the large pressures developed over the relatively short cowl, its angularity might be expected to have significant effects on vehicle thrust and trim. As cowl expansion angle is increased, lower pressures are generated over both cowl and upper wall nozzle surfaces, and as a result the nozzle thrust is somewhat degraded (figure 17a). The most notable effect of cowl angle variation is in the nozzle pitching moment characteristics at the higher Mach numbers. As the cowl angle is initially increased, reduced pressures on the upper wall and cowl surface are essentially compensating and cancel pitching moment variations. Further expansions of the cowl to twelve degrees, however, lowers cowl pressures without a corresponding change on upper wall surfaces and resulting in a net positive pitching moment (figure 17b). Integration of these nozzle forces with the vehicle, however, shows that superior performance levels over most of the Mach number range are achieved with the six degree cowl angle which most nearly balances net engine moments (figure 18). These favorable trim conditions are reflected in the minimal elevon deflections required for the six degree

cowl when compared to larger or smaller cowl angles.

Nozzle cowl length variation.- The length of the baseline nozzle cowl ($L_S/E = 3.12$) extends to a position somewhat beyond the initial expansion wave from the upper wall corner. As shown in figure 19a the position at which this expansion fan strikes the cowl surface results in a sudden drop in cowl pressure approximately three throat heights ($L_S/E \simeq 3$) downstream of the nozzle throat. The baseline nozzle cowl ($L_S/E \simeq 3.12$) was varied by shortening the cowl such that it did not extend to the initial expansion fan and also by lengthening it to extend further into the expansion fan pressure field. As seen in figure 19b, the penalty for not containing all of the high pressure flow as a result of using a short cowl was a drastic reduction in nozzle thrust brought about by lowered cowl thrust forces and by reduced upper wall pressures induced by a premature expansion fan from the cowl trailing edge. For this case nozzle upper wall lift forces are much larger than the short cowl negative lift force and a large negative nozzle pitching moment is induced at Mach 10. Extending the nozzle cowl, however, has a beneficial effect on net nozzle thrust throughout the Mach number range and produces a net positive nozzle pitching moment increment compared to the reference nozzle.

It was shown in the Scramjet Location section, that increasing cowl length past the reference nozzle cowl length of 3.12 does slightly increase nozzle thrust and vehicle thrust margin capability at Mach 10. That the same trend extends through Mach 4 is shown in figure 20. Differences between power-on and power-off trim elevon deflections also decrease for the longer cowl length. More detailed tradeoffs between cowl weight, cooling requirements and propulsion efficiency will be required to ultimately select the optimum cowl length. However, in view of the small performance gains which result from increased cowl

lengths, the final cowl length may be relatively short.

VEHICLE PERFORMANCE - PROPULSION

The previous sections which focused on parametric variations of nozzle geometry and engine location determined that for the research vehicle of this study the baseline nozzle was near optimum under all conditions studied. This baseline nozzle will now be used to briefly assess propulsion effects on vehicle stability and acceleration. Results will reflect integrated totals of forebody inlet compression, spillage, engine module and nozzle efficiency and trimmed aircraft aerodynamics through changes in angle-of-attack.

Longitudinal stability.- The addition of scramjet modules power-on or power-off has a mixed although small effect on vehicle stability as shown in figure 21 for trimmed accelerating flight. For example, engine power affects on stability at Mach 10 has a destabilizing influence at low angles of attack and a stabilizing effect at higher angles. Basic airframe stability parameters (aerodynamic center location) were computed as previously described using simplified methods which generally predict aerodynamic centers forward of their true position. However, the implications of this stability analysis is that for a well designed engine nozzle combination, longitudinal characteristics of this type of basic airframe will not be seriously affected by the addition of scramjet engine modules, either power-off or power-on.

Elevon deflections required for trim at angle of attack are shown in figure 22. The maximum elevon deflection needed from power-on to power-off conditions is eight degrees which should be within acceptable limits; however, the dynamic behavior of such a vehicle in an engine shutdown situation is unknown and warrants further study.

Acceleration performance.- The nozzle parametric investigations of the preceding sections of this paper have led to the conclusion that for accelerating flight a large expansion nozzle with moderate cowl lengths and cowl deflection angles correctly located aft of the aircraft center of gravity position provides superior acceleration performance at two degrees angle of attack. Of course, realistic acceleration trajectories will deviate somewhat from such a constant angle of attack.

The ability to resolve total vehicle forces into orthogonal lift and drag (thrust) vectors allows us to investigate acceleration performance through an angle of attack range using as a first order criteria of merit the following relation derived from a simple vehicle force analysis at small flight path angles.

$$\text{Acceleration} = K[(T-D)/D]/[(L/D)/(1-\frac{V^2}{V_S^2})]$$

Thrust and drag vectors are orthogonal to the lift vector and K is a constant of proportionality. The first component of this equation, the thrust margin ((T-D)/D),is examined in some detail in figure 23 which shows angle of attack effects on thrust and drag components for the trimmed research vehicle at Mach 10. As angle of attack increases, nozzle and engine module thrust increases primarily as a result of increased mass flow ingested by the engine inlet and secondarily due to the greater cycle efficiency associated with reduced inlet Mach numbers. Aircraft drag typically increases with angle of attack due to increased vehicle wave drag. Thrust margin [(T-D)/D], however, peaks near two degrees angle of attack as a result of the interplay between increased engine and nozzle thrust at angle of attack versus increasing aerodynamic drag at these higher angles. This result is shown on the thrust margin curves at the top of

figure 24. These same figures also show that at lower Mach numbers maximum thrust margins also peak at low angles of attack.

Figure 24 also presents the lift-drag ratio terms contained in the acceleration equation. These integrated lift-drag ratios are summations of aerodynamic and all propulsion forces in the lift direction and are corrected for centrifugal effects. These ratios tend to peak at higher angles of attack than the thrust margins. As shown in the lower portion of figure 24 maximum acceleration occurs at low angles of attack (high dynamic pressures) where minimum drag coefficients and good thrust margins occur. The practical limit of this trend must be commensurate with heating and structural limitations on dynamic pressure which correspond to a 71,850 n/m^2 (1500 psf) acceleration trajectory for this research airplane concept.

CONCLUDING REMARKS

A preliminary study was conducted of scramjet engine-nozzle integration at hypersonic speeds and the results of the analysis were applied to a highly integrated hypersonic research aircraft. As a result of the perturbation of major engine-airframe design parameters, several encouraging conclusions regarding scramjet-airframe integration have resulted. Foremost of these is that with proper design, an efficient fixed geometry engine-nozzle combination using the aircraft afterbody as an exhaust nozzle, provides controlled and stable flight over a wide range of Mach numbers. The relative simplicity inherent in fixed geometry nozzle concepts combined with fixed geometry engine modules as compared with variable geometry systems should facilitate

future scramjet propulsion system development. Also significant from a total vehicle performance standpoint was the result that nozzle designs which optimize at the high speed end of the flight envelope also generally show superior performance at the low speed end of the scramjet operating range. Thus, only a small penalty must be paid in nozzle performance at any Mach number for the fixed geometry concept. For vehicle types similar to the one studied in this paper, only slight changes in basic aircraft stability are anticipated with the addition of engine modules to the vehicle undersurface and no major effect on power-on conditions was noted on longitudinal stability.

Due to the preliminary nature of the study only major design trends were developed and many important, though second-order parameters, were not considered. In particular the sensitivity of nozzle design to three-dimensional flow variations was not assessed but should be included in more detailed future investigations. Future work must also be carried out in the area of vehicle dynamic behavior and control effectiveness during an engine shutdown situation. Although this study showed only moderate changes in elevon trim requirements between power-on and power-off engine conditions, the overall vehicle dynamic performance under such transient conditions is unknown.

REFERENCES

1. Becker, John V.; and Kirkham, Frank S.: Hypersonic Transports. NASA SP-292, Paper No. 25, Nov. 1971, pp. 429-445.
2. Nagel, A. L.; and Becker, J. V.: Key Technology for Airbreathing Hypersonic Aircraft. Presented at the AIAA 9th Meeting and Technical Display, Washington, D. C., Jan. 1973.
3. Becker, J. V.: New Approaches to Hypersonic Aircraft. Seventh Congress of the International Council of the Aeronautical Sciences, Rome Italy, Sept. 14-18, 1970.
4. Small, W. J.; Fetterman, D. E.; and Bonner, T. F., Jr.: Alternate Fuels for Transportation. Part 1: Hydrogen for Aircraft. Mechanical Engineering, May 1974, pp. 18-24.
5. Gregory, Thomas J.; Williams, Louis J.; and Wilcox, Darrell E.: The Airbreathing Launch Vehicle for Earth Orbit Shuttle - Performance and Operation. Presented at AIAA Advanced Space Transportation Meeting, Feb. 4-6, 1970.
6. Johnston, P. J.; Cubbage, J. M.; and Weidner, J. P.: Studies of Engine-Airframe Integration on Hypersonic Aircraft. AIAA Paper No. 70-542, May 1970.
7. Cubbage, J. M.; and Kirkham, F. S.: Investigation of Engine-Exhaust-Airframe Interference on a Cruise Vehicle at Mach 6. NASA TN D-6060.
8. Kirkham, F. S.; Cubbage, J. M.; Vahl, W. A.; and Small, W. J.: Studies of Airframe-Propulsion-System Integration for Mach 6 Cruise Vehicles. NASA TN D-4128.

9. Anderson, G. Y.: An Examination of Injector/Combustor Design Effects on Scramjet Performance. Presented at the 2nd International Symposium on Air Breathing Engines, Sheffield, England, March 25-29, 1974.

10. Edwards, C. L. W.: A Forebody Design Technique for Highly Integrated Bottom-Mounted Scramjets with Application to a Hypersonic Research Airplane. NASA TM X-71971, Nov. 1974, Langley Research Center, Hampton, VA.

11. Kirkham, F. S., and Driver, C.: Liquid Hydrogen Fueled Aircraft - Prospects and Design Issues. AIAA Paper No. 73-809, presented at the AIAA 5th Aircraft Design, Flight Test and Operations Meeting, St. Louis, Missouri, Aug. 1973.

12. Henry, J. R.; and Beach, H. L.: Hypersonic Airbreathing Propulsion Systems. NASA SP-292, Paper No. 8, Nov. 1971, pp. 157-172.

13. Henry, J. R.; and Anderson, G. Y.: Design Considerations for the Airframe-Integrated Scramjet. NASA TM X-2895, 1973.

14. Gentry, A. E.; and Smyth, D. N.: Hypersonic Arbitrary-Body Aerodynamic Computer Program (Mark III version). Rep. DAC61552 (Air Force Contract Nos. F3361567C1008 and F3361567C1602), Douglas Aircraft Co., April 1968. Vol. I User's Manual. (Available from DDC as AD 851811). Vol II - Program Formulation and Listings. (Available from DDC as AD 8511812).

15. Jackson, Robert J.; and Wang, Tennyson T.: Computer Program Description, Ramjet and Scramjet Cycle Performance. NASA CR-132-454, 1974.

16. Dash, S.; Del Guidice, P.; and Kalben, P.: Analysis and Design of Three-Dimensional Supersonic Nozzles. NASA CR 132350, Vol. I and II, 1972.

TABLE 1 - ENGINE INLET AND COMBUSTOR EXIT CONDITIONS, $\alpha = 2°$, $q_\infty = 71850 n/m^2$

M_∞	ϕ	P_1, n/m^2	T_1, °K	V_1, m/sec	P_3, n/m^2	T_3, °K	V_3, m/sec	OPERATIONAL MODE
4	1.0	10366	244	1153	157717	2343	1093	RAMJET
↓	0	↓	↓	↓	17888	338	1072	↓
6	1.0	6248	282	1753	101027	2328	1621	SCRAMJET
↓	0	↓	↓	↓	16327	448	1655	↓
10	1.5	3840	353	2982	57935	2222	2837	SCRAMJET
↓	0	↓	↓	↓	14172	772	2831	↓

TABLE 2 - ISOLATED LIFT DRAG AND MOMENT COEFFICIENTS

NOTES:

1. "A" Point of application of forces.
2. Free stream pressure has been subtracted from all surfaces prior to integrations.

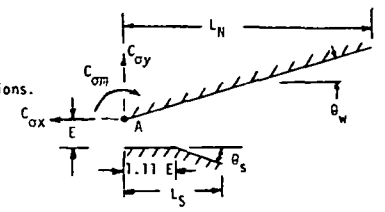

$C_{oy} = \frac{\text{Lift}}{q_\infty A_c}$

$C_{ox} = \frac{\text{Thrust}}{q_\infty A_c}$

$C_{om} = \frac{\text{Moment}}{q_\infty A_c L_N}$

$M_\infty = 4$

θ_W	L_N/E	θ_S	L_S/E	ϕ	C_{oy}	C_{ox}	C_{om}	P_∞/q
6.52	18.54	6.00	3.12	0.	-.536	-.015	.352	.0893
				1.0	1.966	.823	-.559	
12.02				0.	-1.021	-.1406	.547	
				1.0	1.033	.994	-.272	
19.8		0.		0.	-1.467	-.358	.655	
				1.0	-.044	1.107	.149	
		6.0	1.50	0.	-1.353	-.412	.737	
				1.0	.172	.802	.090	
			3.12	0.	-1.442	-.397	.744	
				1.0	-.138	1.065	.009	
			4.50	0.	-1.455	-.394	.747	
				1.0	-.325	1.113	.010	
		12.0	3.12	0.	-1.347	-.418	.752	
				1.0	-.090	1.041	.085	

$M_\infty = 6.0$

θ	L_N/E	θ_S	L_S/E	ϕ	C_{oy}	C_{ox}	C_{om}	P_∞/q
6.52	18.54	6.0	3.12	0.	.157	.076	.061	.0397
				1.	2.740	.777	-1.077	
12.02				0.	-.338	.022	.108	
				1.	1.643	1.043	-.775	
19.8		0.		0.	-.934	-.129	.269	
				1.	.186	1.183	-.631	
		6.	1.50	0.	-.645	-.169	.270	
				1.	.795	.944	-.468	
			3.12	0.	.771	-.128	.284	
				1.	.371	1.203	-.524	
			4.50	0.	-.871	-.114	.300	
				1.	-.054	1.241	-.497	
		12.0	3.12	0.	-.657	-.138	.275	
				1.	.280	1.167	-.420	

$M_\infty = 10$

θW	L_N/E	θ_S	L_S/E	ϕ	C_{oy}	C_{ox}	C_{om}	P_∞/q
6.52	18.54	6.00	3.12	0.	.431	.103	-.244	.0143
				1.5	2.260	.575	-1.069	
12.02				0.	-.062	-.075	.083	
				1.5	1.217	.757	.838	
14.83	27.02		1.50		1.565	.706	-.605	
			3.12		.996	.864	-.862	
			4.50		.556	.928	-.687	
19.8	18.54	0	3.12	0.	-.656	-.0338	.109	
				1.5	-.090	.796	-.705	
		6.0	1.50	0.	-.329	-.0336	-.0771	
				1.5	.703	.644	-.563	
			3.12	0.	.443	-.0192	.087	
				1.5	.102	.811	-.607	
			4.50	0.	-.545	-.008	.108	
				1.5	-.351	.845	-.501	
		12.0	3.12	0.	-	-	-	
				1.5	.208	.761	.475	
28.66	11.26	6.0	1.50		-.228	.462	-.395	
			3.12		-1.047	.548	-.219	
			4.50		-1.470	.592	-.074	

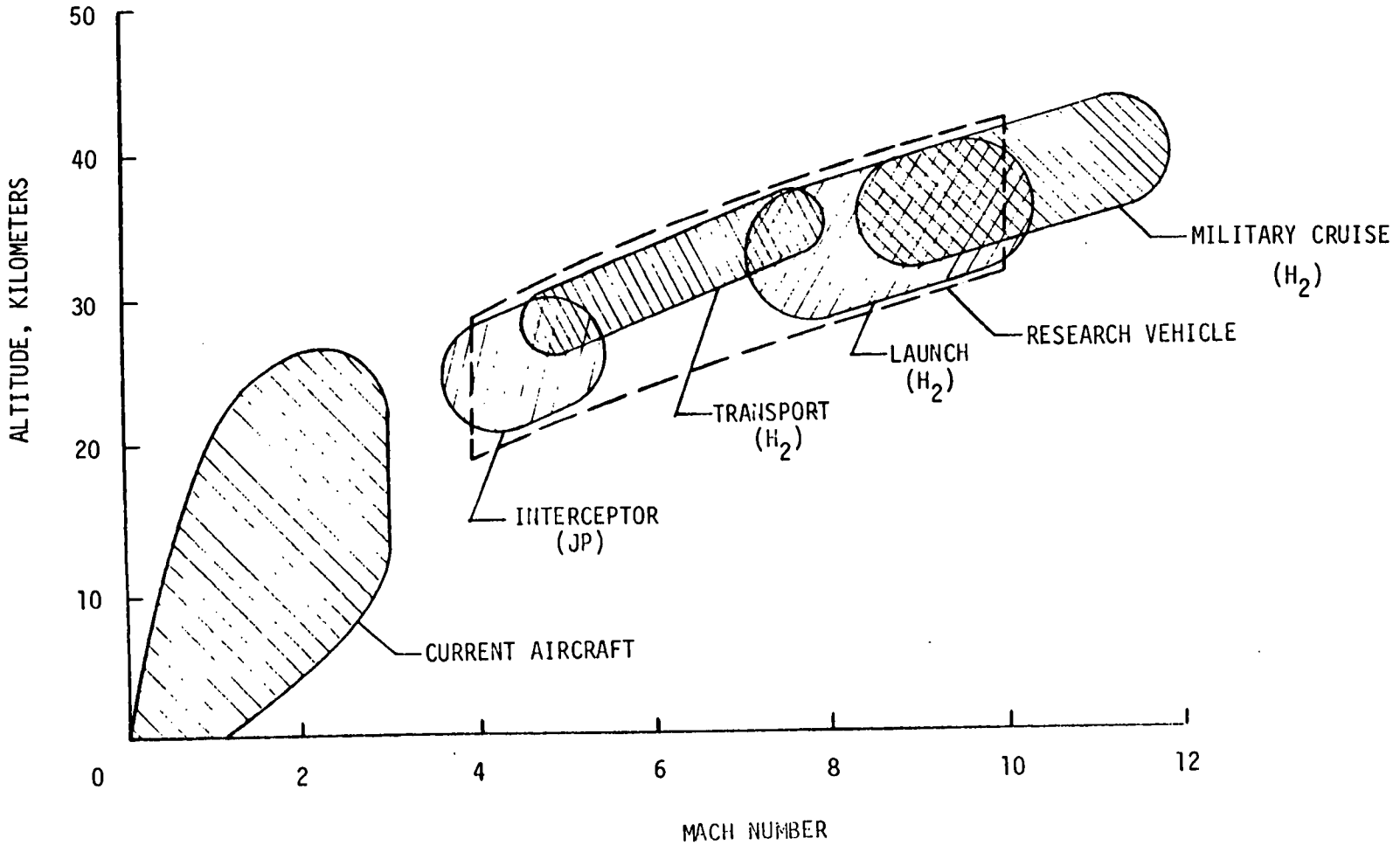

Figure 1.- Hypersonic flight envelope.

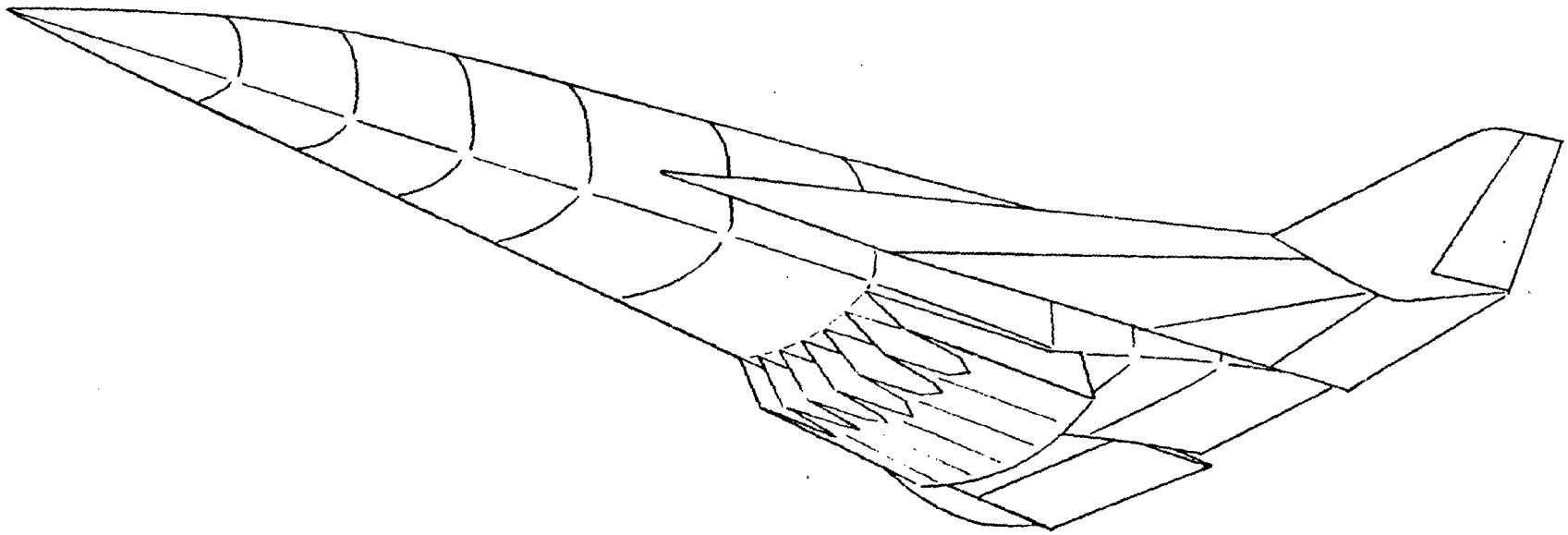

Figure 2.- Hydrogen-fueled research airplane.

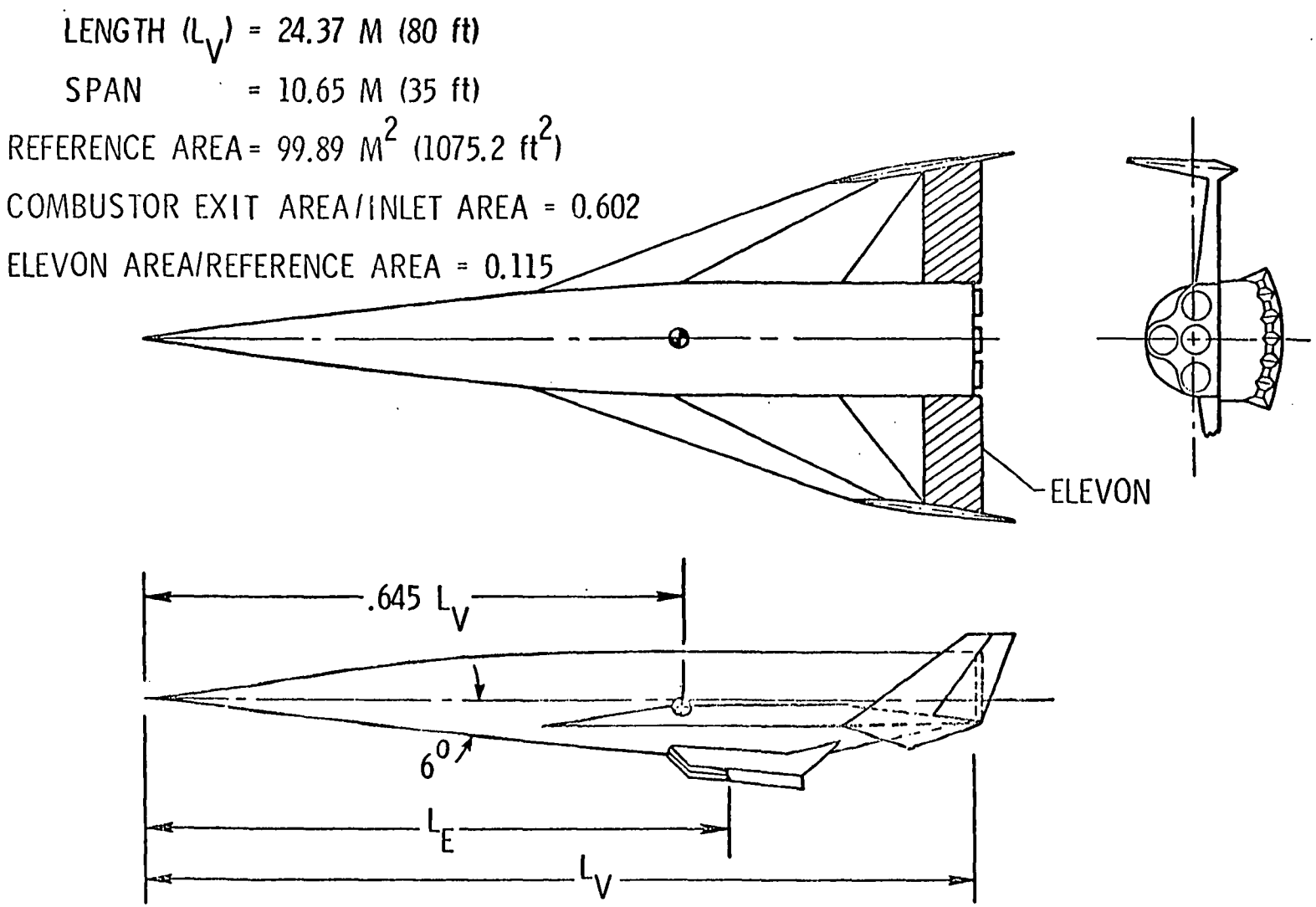

Figure 3.- Hydrogen-fueled research airplane concept.

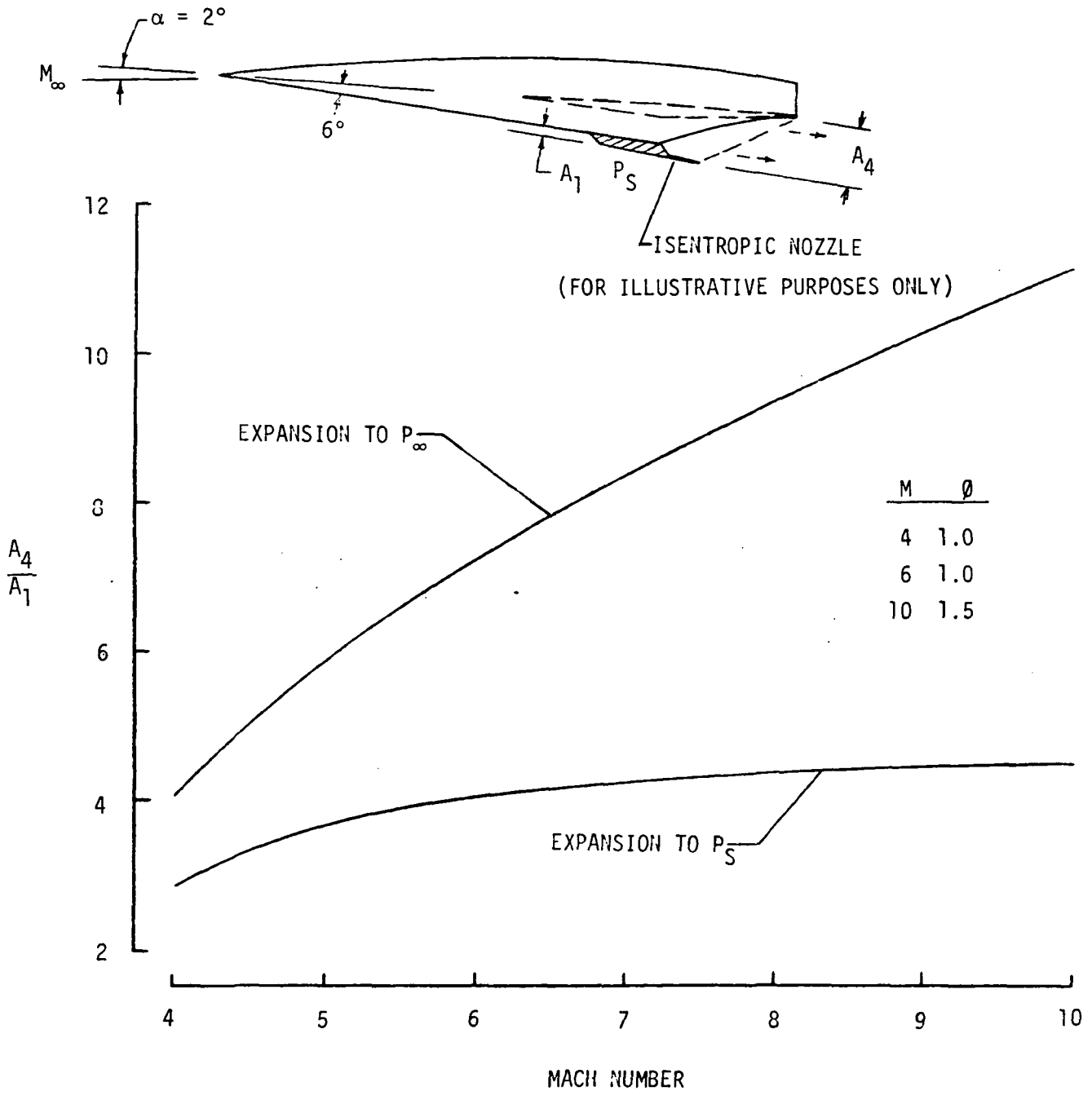

Figure 4.- Ideal nozzle area expansion hydrogen-air combustion products chemical equilibrium, q_∞ = 71850 N/M^2 (1500 psf).

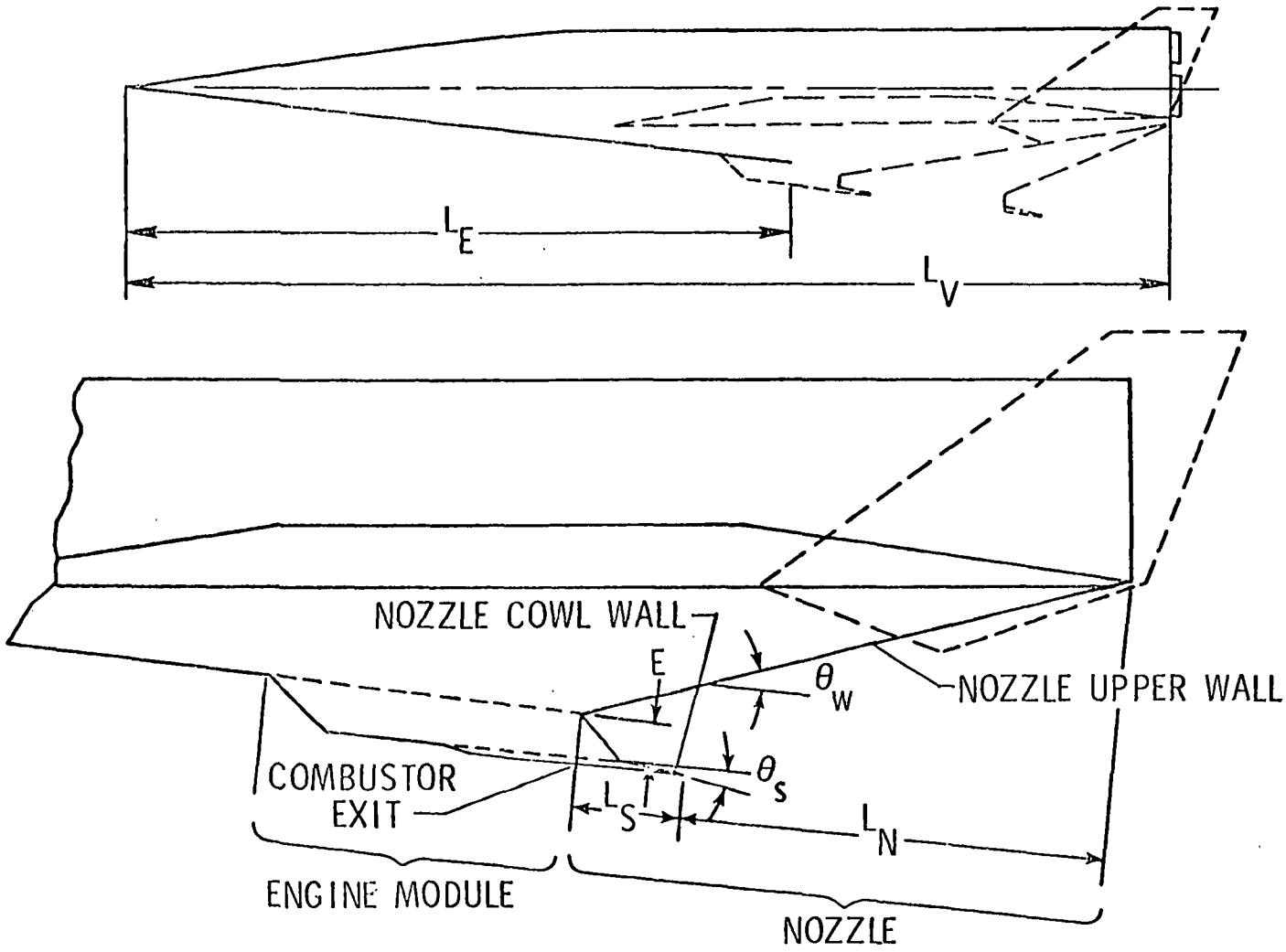

Figure 5.- Key nozzle optimization variables.

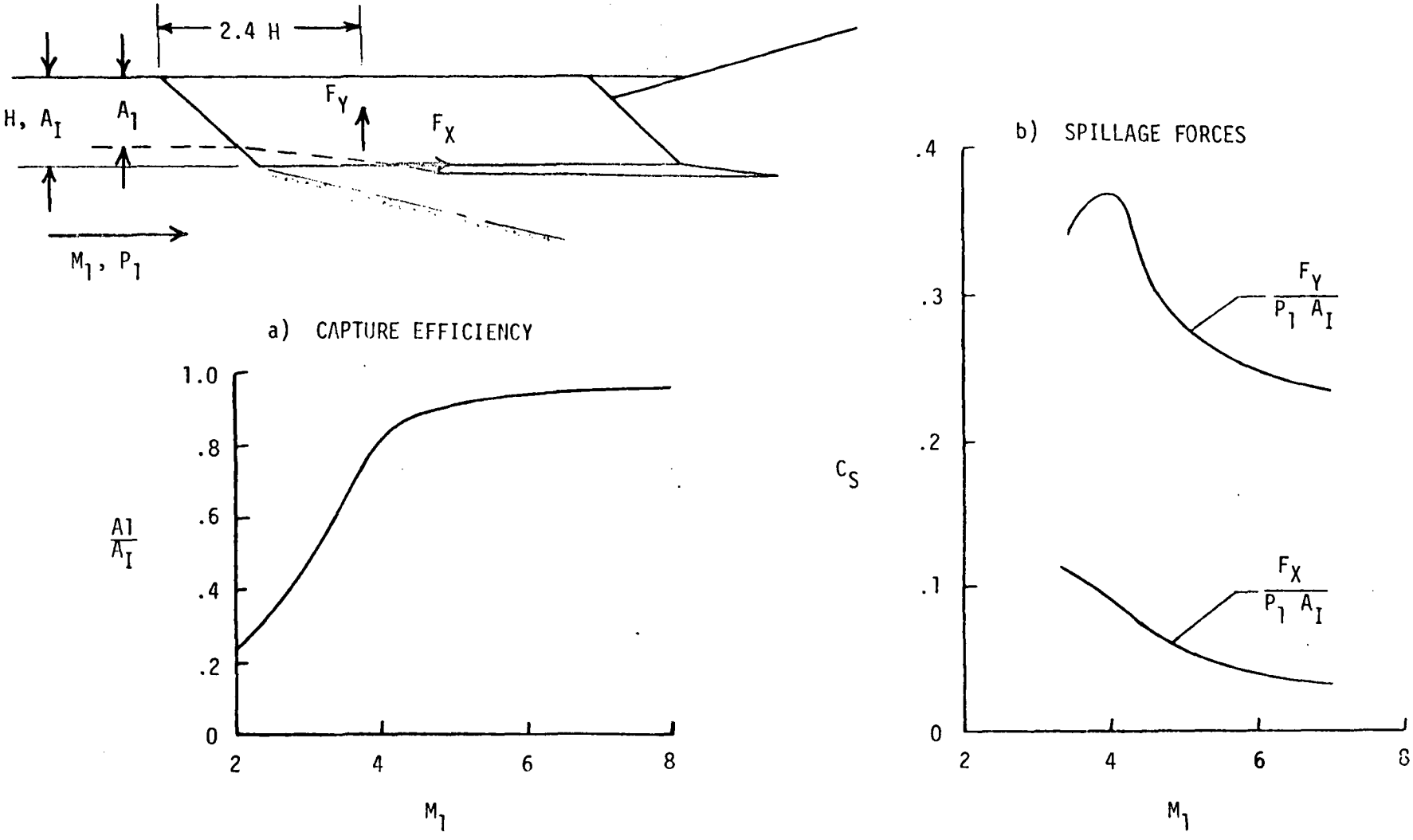

Figure 6.- LRC scramjet inlet capture performance estimates.

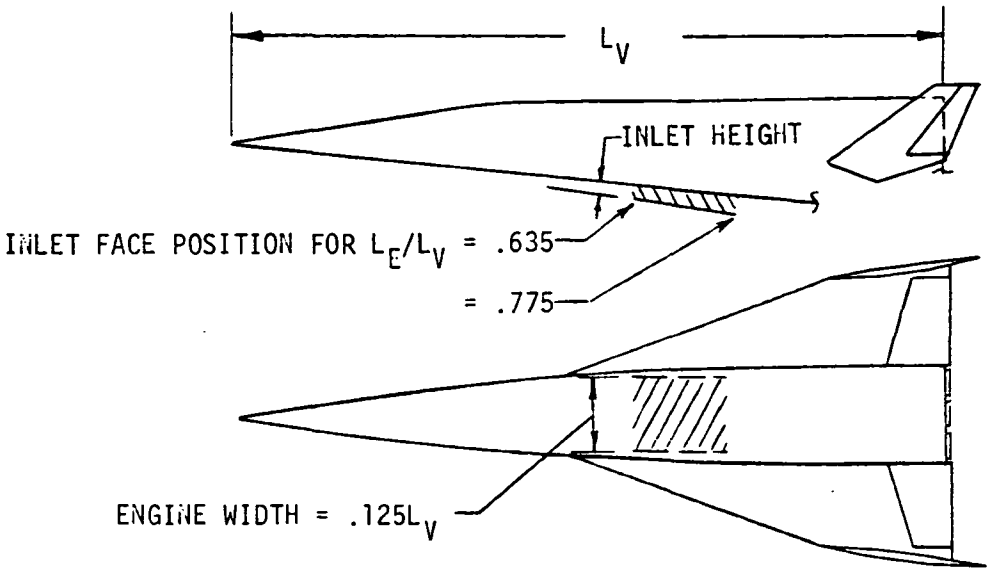

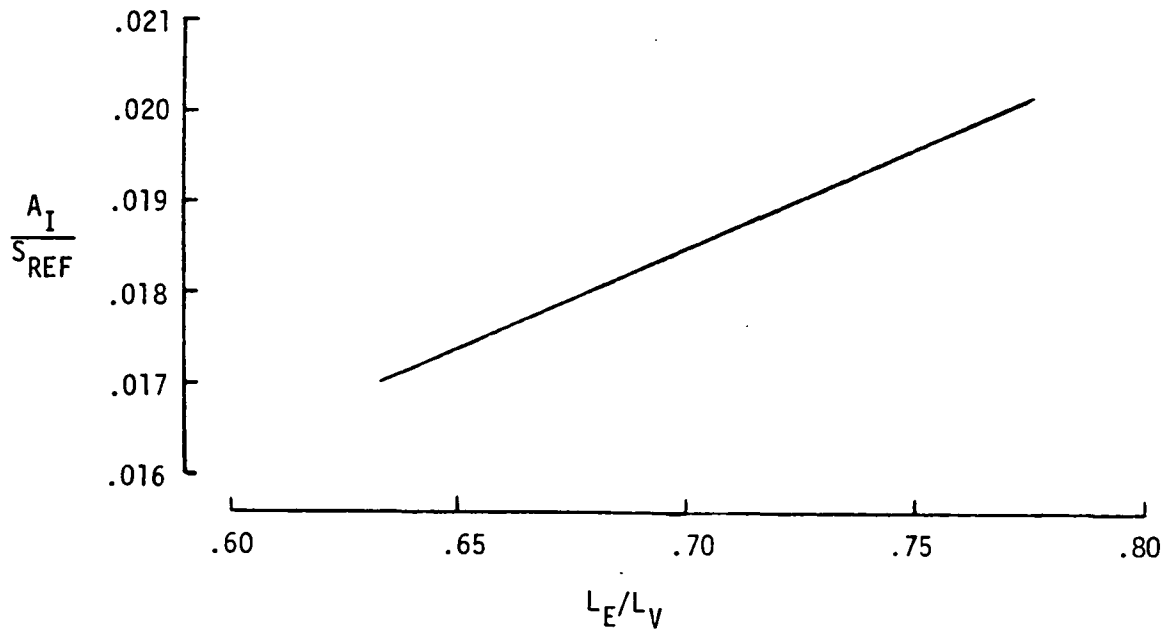

Figure 7.- Inlet area variation along body length.

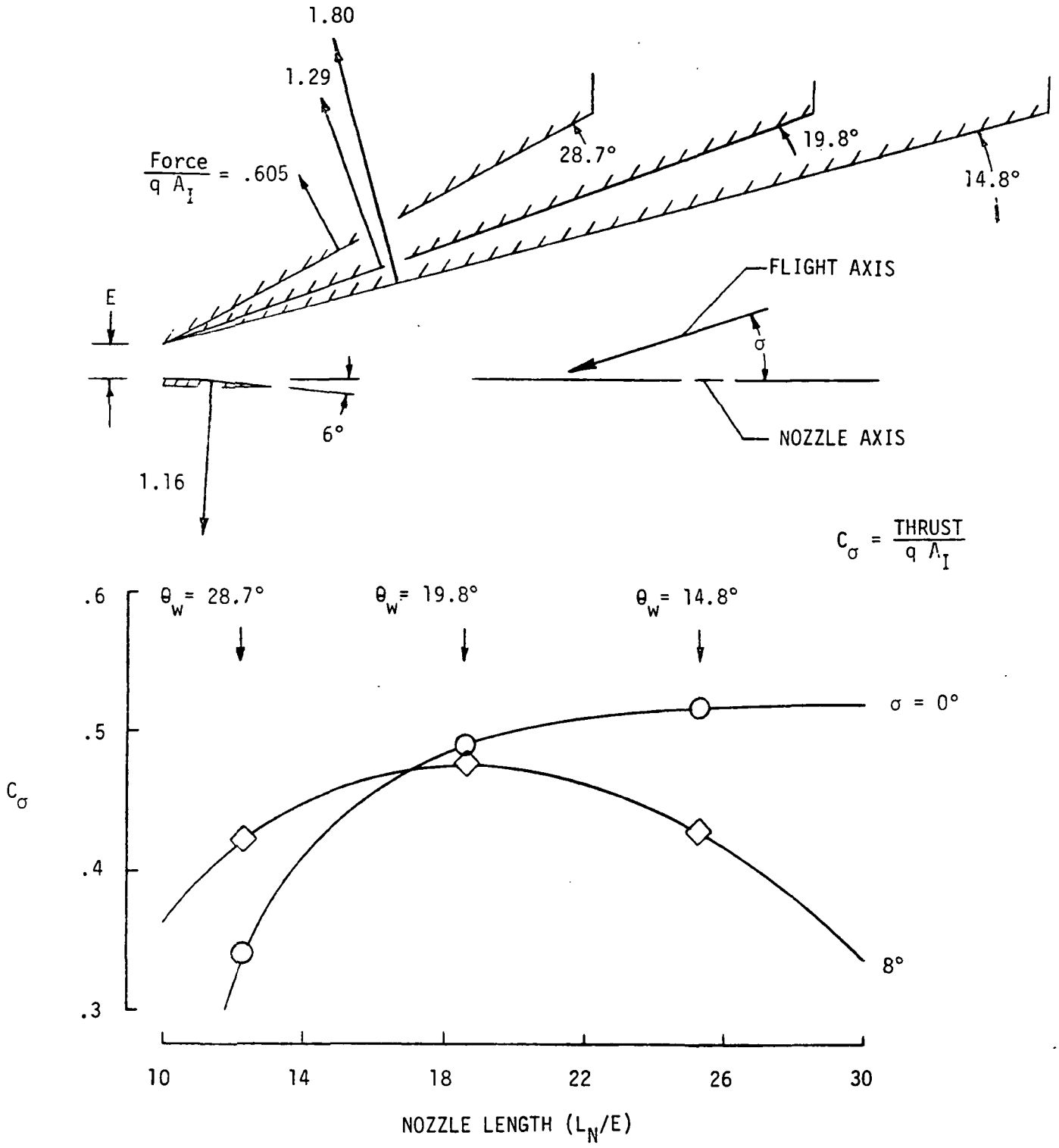

Figure 8.- Isolated nozzle force characteristics, M_∞ = 10, q = n/m^2 (1500 psf), $\emptyset$ = 1.5, L_S/E = 3.12

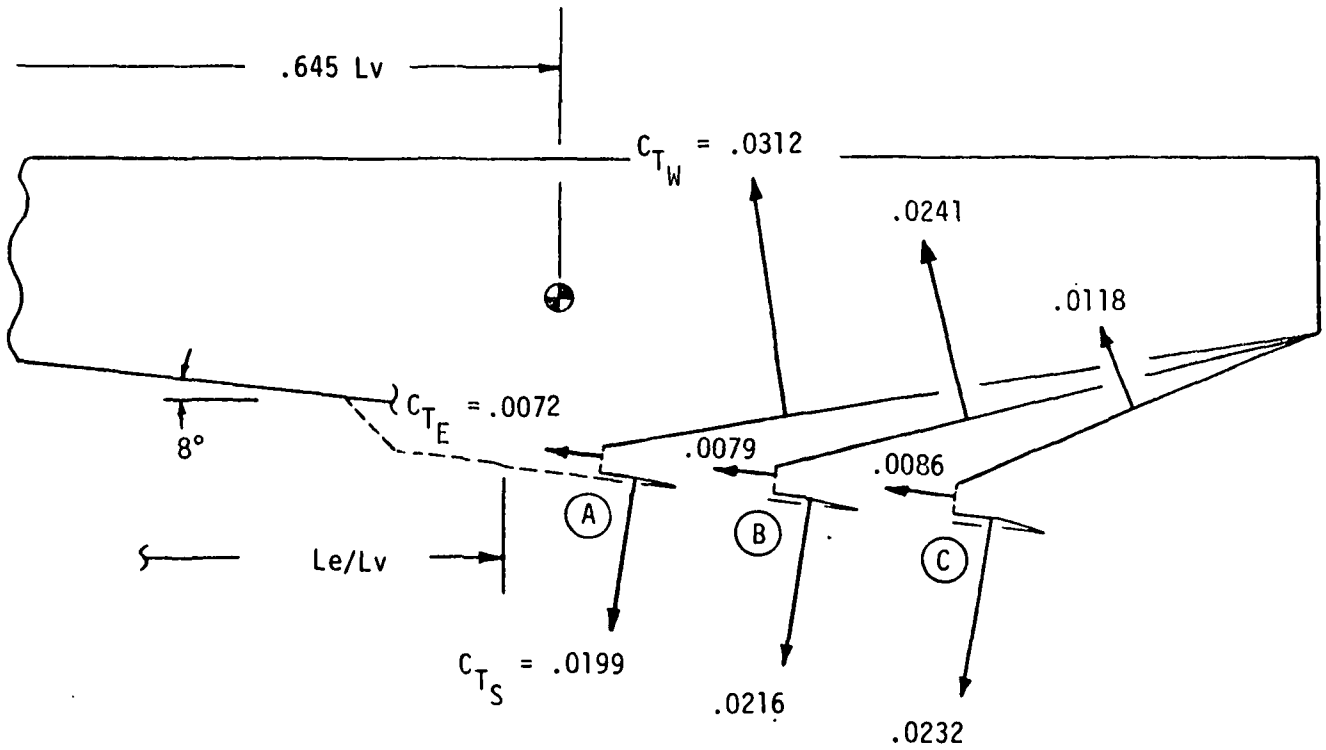

NOZZLE	Le/Lv	θw	θs
(A)	.635	14.8	6.
(B)	.694	19.8	6.
(C)	.775	28.7	6.

Figure 9.- Propulsion forces, axial scramjet location
M_∞ = 10, α = 2°, q = 71850 n/m^2 (1500 psf).

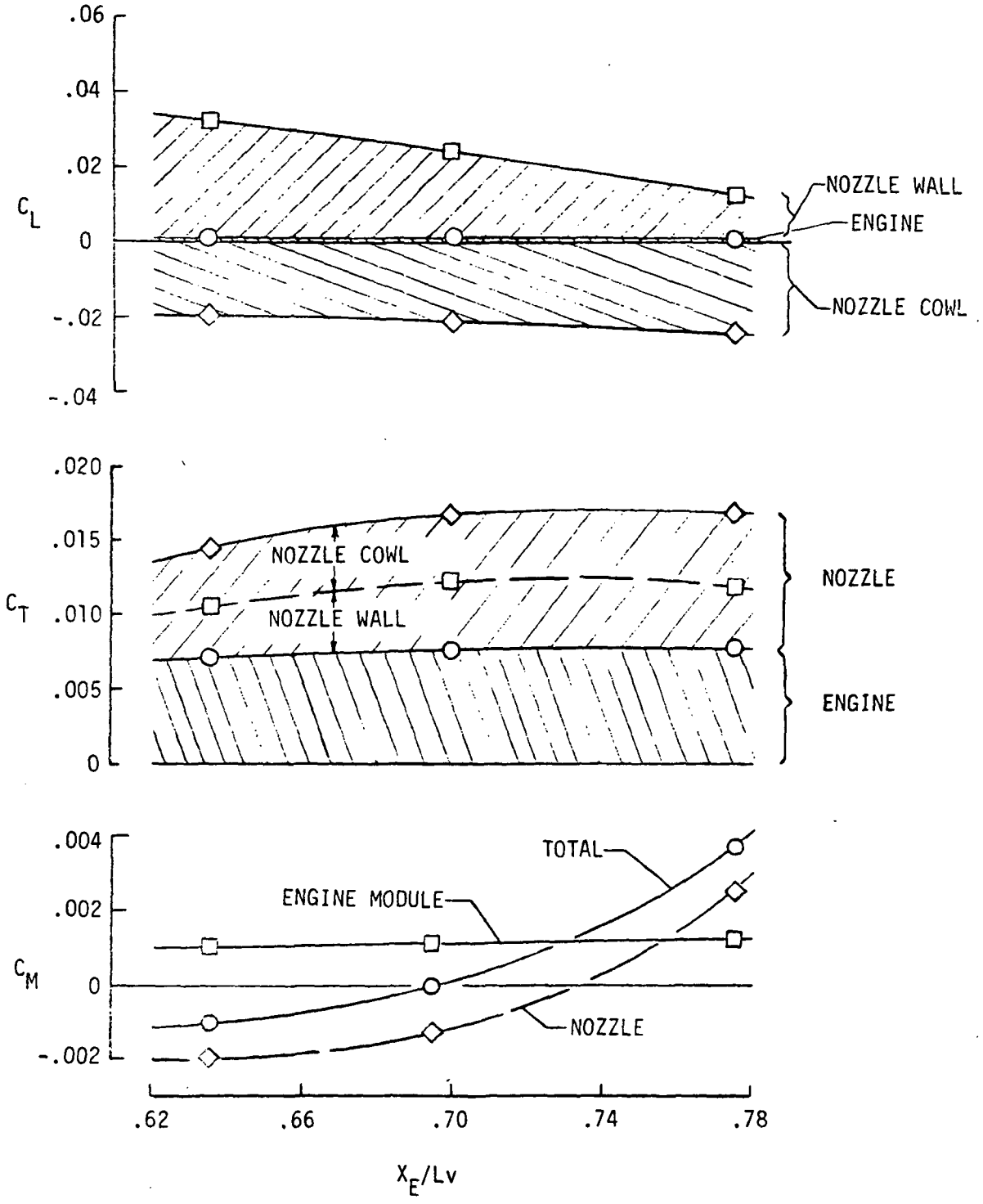

Figure 10.- Variation of scramjet location,
M_∞ = 10, α = 2°, q = 71850 n/m^2 (1500 psf)

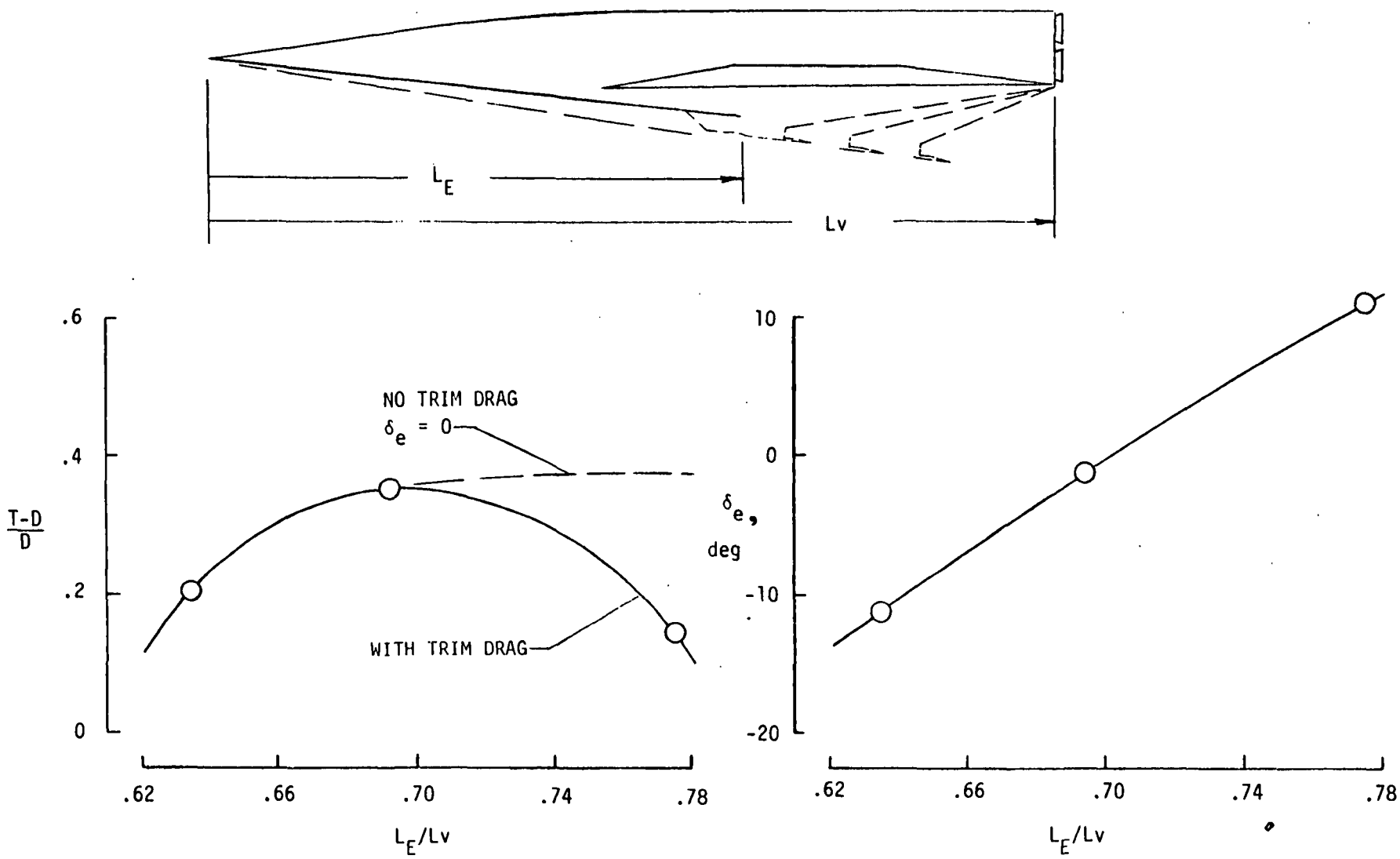

Figure 11.- Engine axial location (integrated effects, M_∞ = 10, q = 71850 n/m2 (1500 psf), α = 2°.

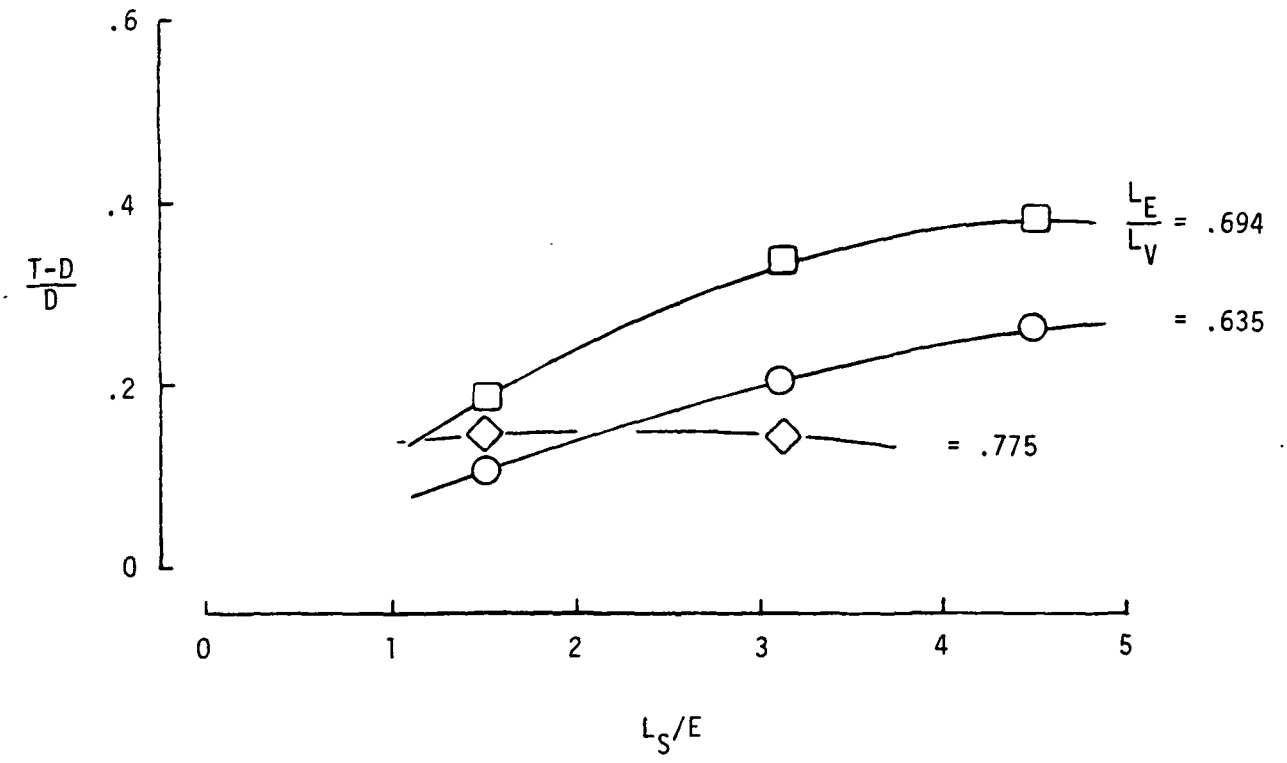

Figure 12.- Engine axial location (cowl length effects), M_∞ = 10, $\emptyset$ = 1.5.

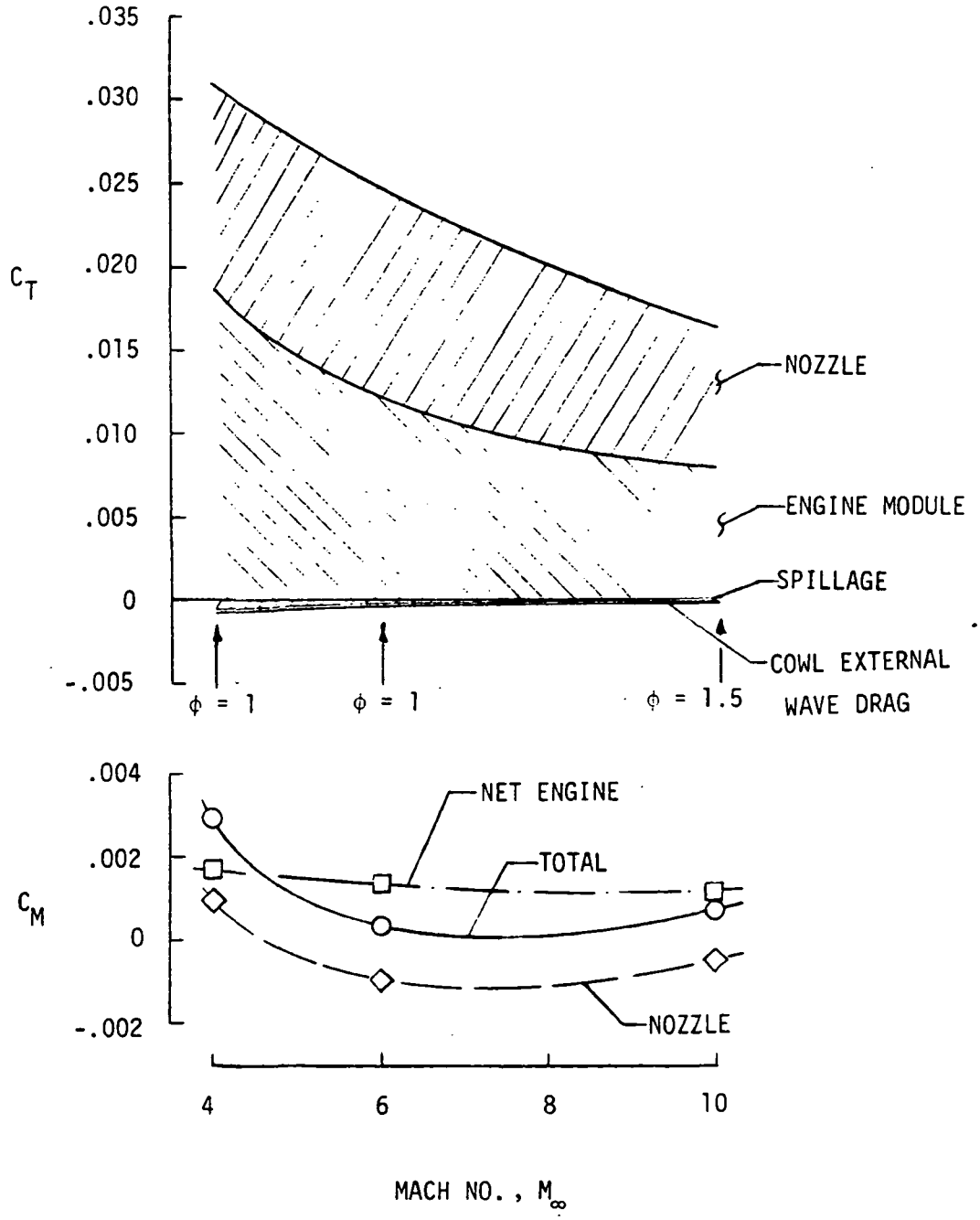

Figure 13.- Engine/nozzle thrust components, $q = 71850\ n/m^2$ (1500 psf), $\alpha = 2.0°$.

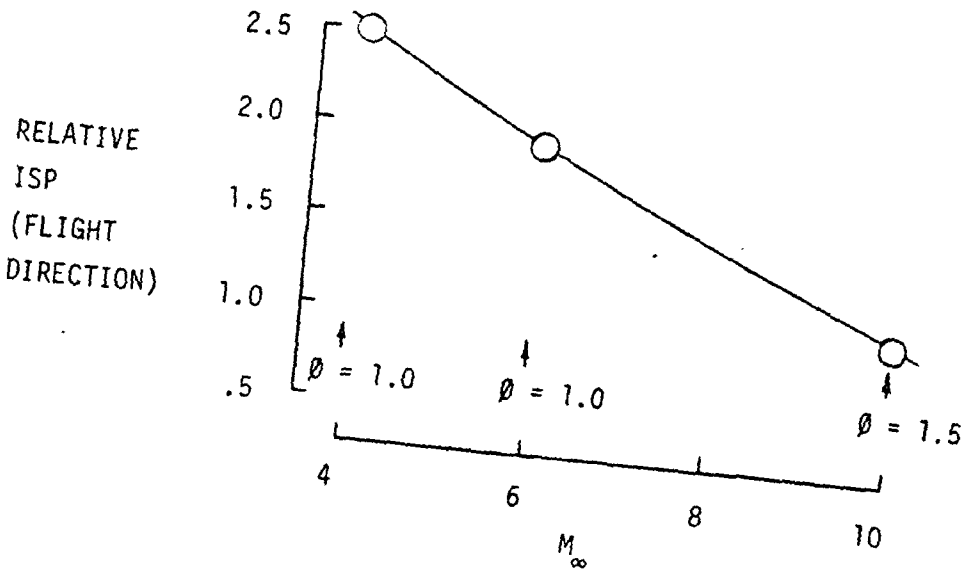

Figure 14.- Propulsion system efficiency, $q = 71850\ n/m^2$ (1500 psf), $\alpha = 2.0°$.

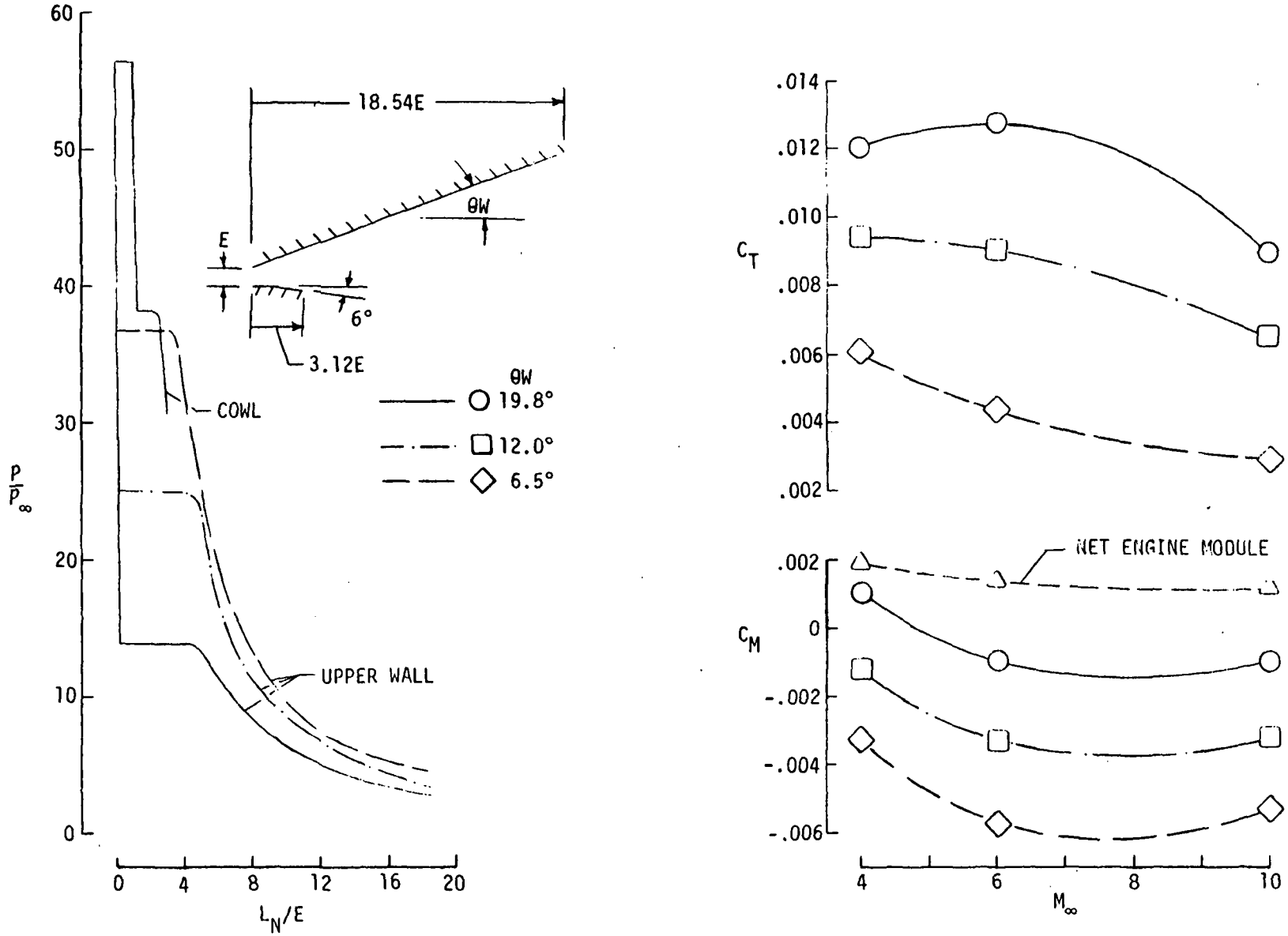

(a) NOZZLE PRESSURE DISTRIBUTIONS $M_\infty = 10$

(b) NOZZLE THRUST AND MOMENTS

Figure 15.- Nozzle wall angle variation, q = 71850 n/m^2 (1500 psf), $\alpha = 2°$.

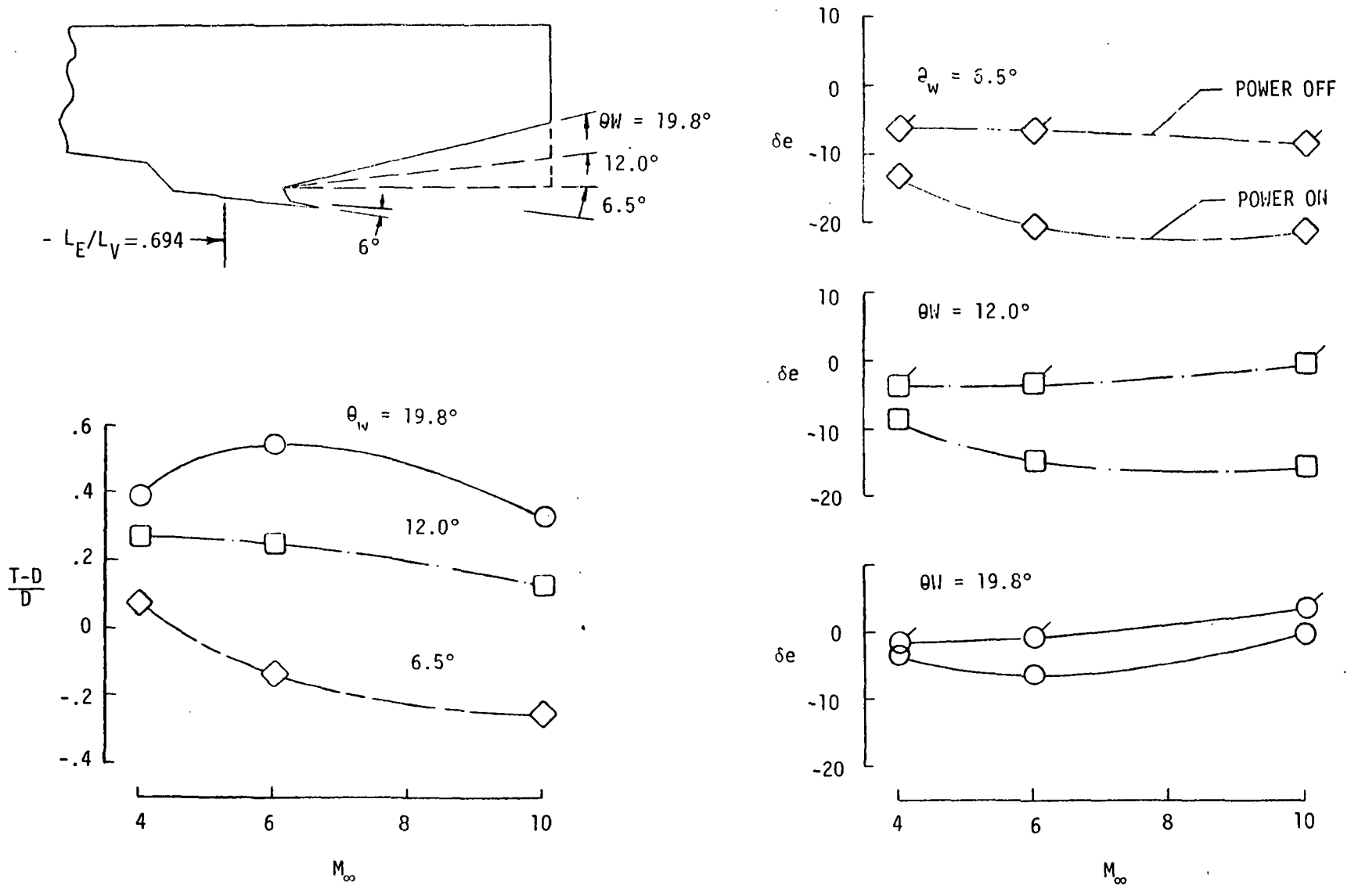

Figure 16.- Nozzle expansion effects,
q = 71850 n/m^2 (1500 psf), α = 2°.

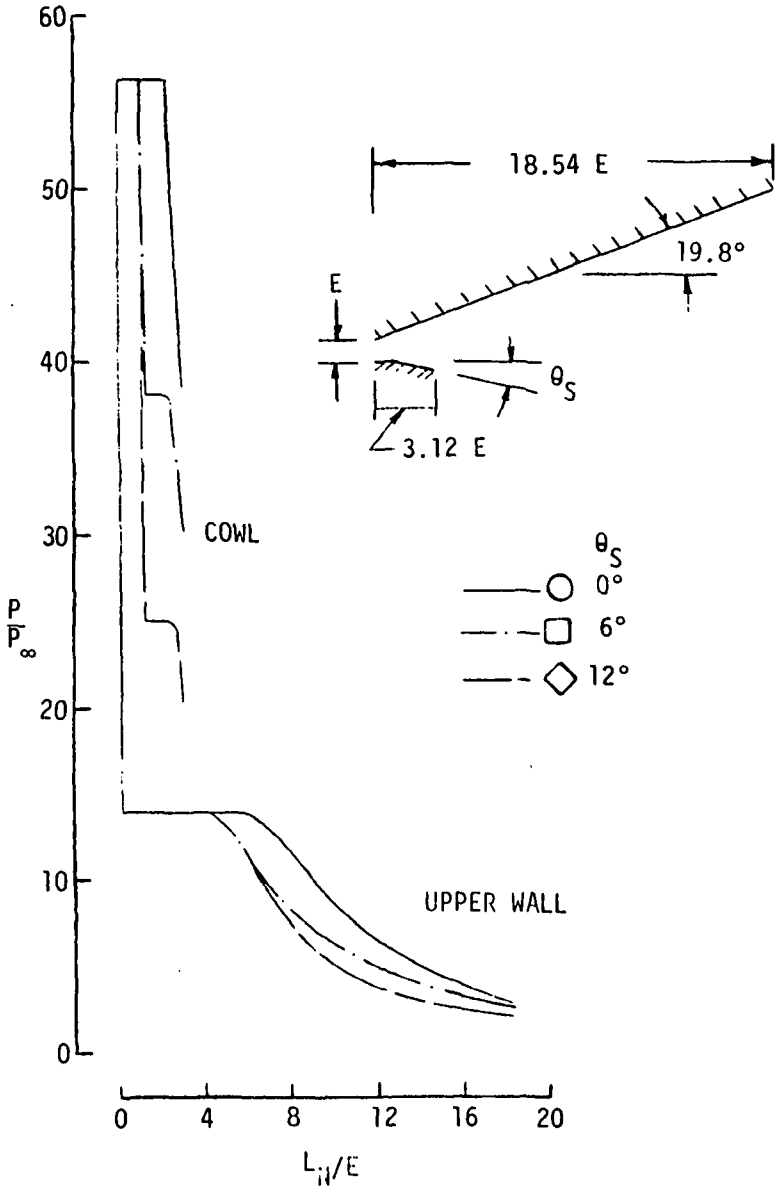

(a) NOZZLE PRESSURE DISTRIBUTION, M_∞ = 10

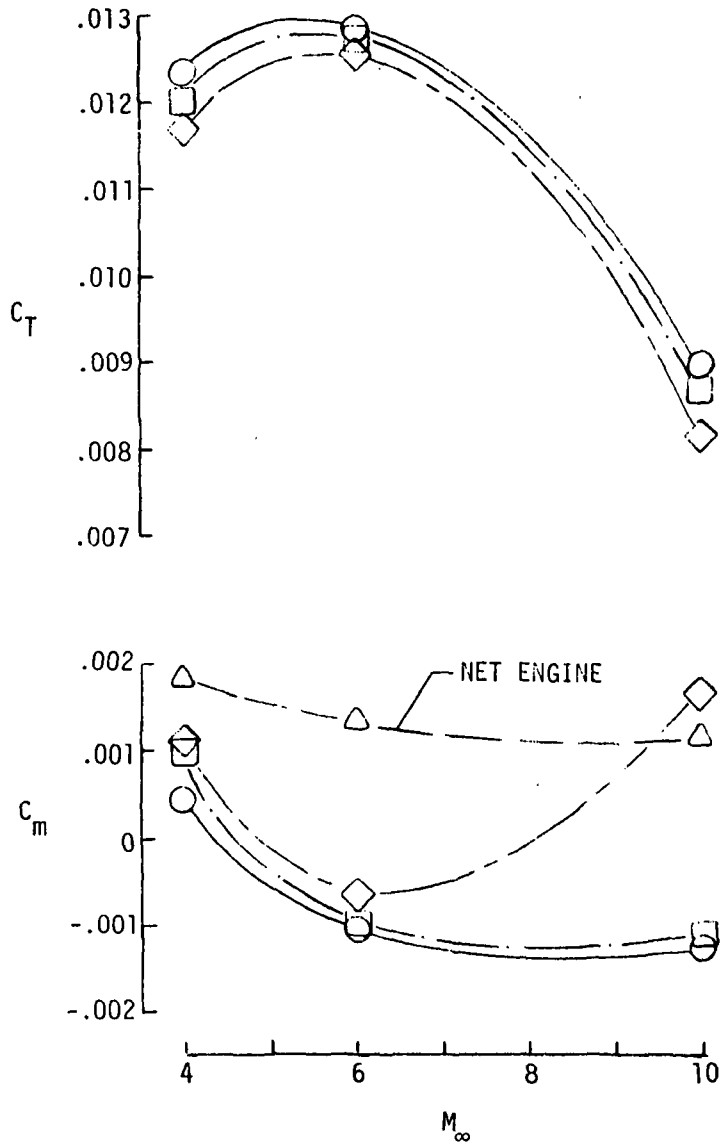

(b) NOZZLE THRUST AND MOMENTS

Figure 17.- Nozzle cowl angle variation, q = 71850 n/m^2 (1500 psf), α = 2°.

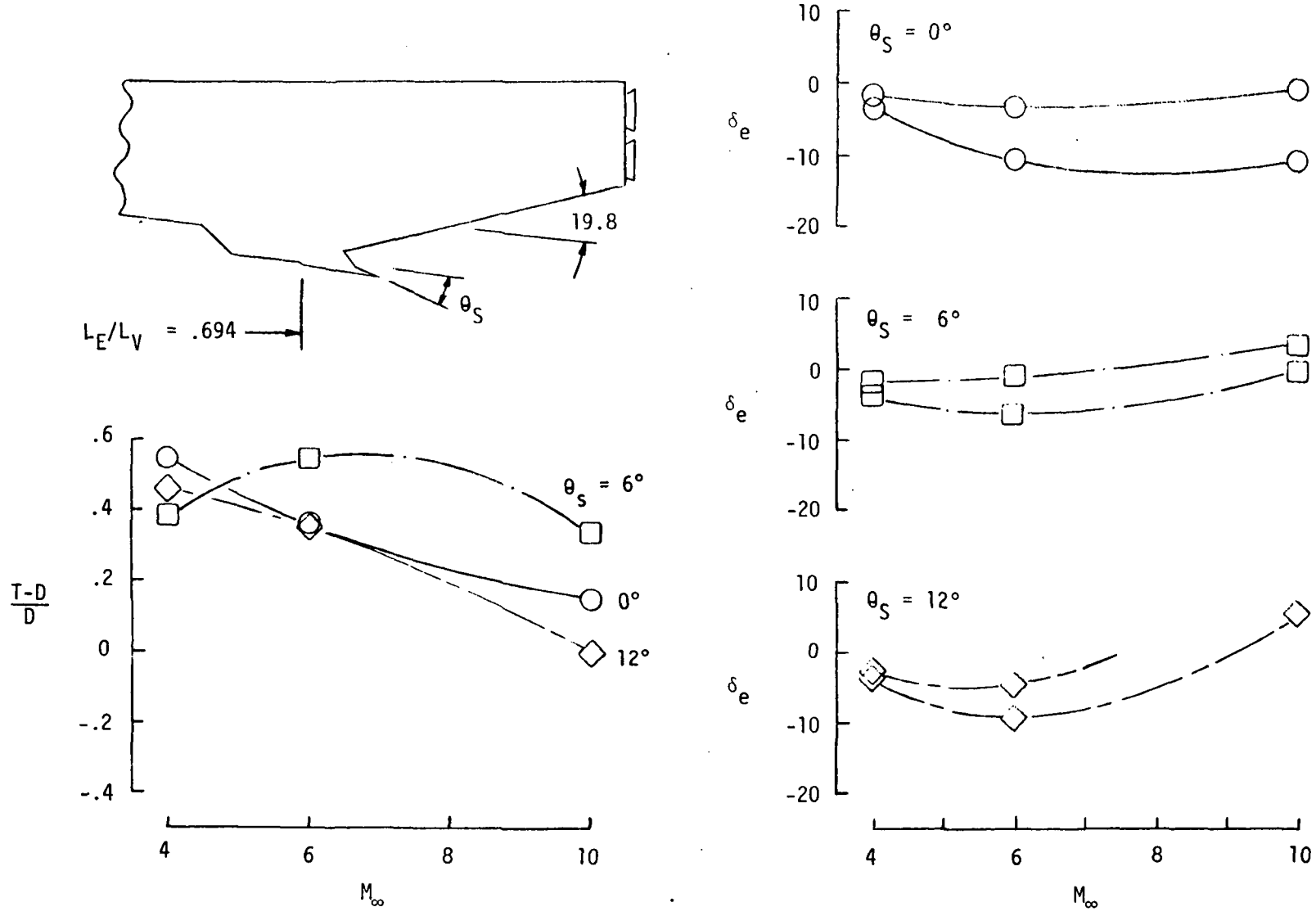

(a) THRUST MARGIN

(b) ELEVON TRIM DEFLECTIONS

Figure 18.- Nozzle cowl angle variation, q = 71850 n/m^2 (1500 psf).

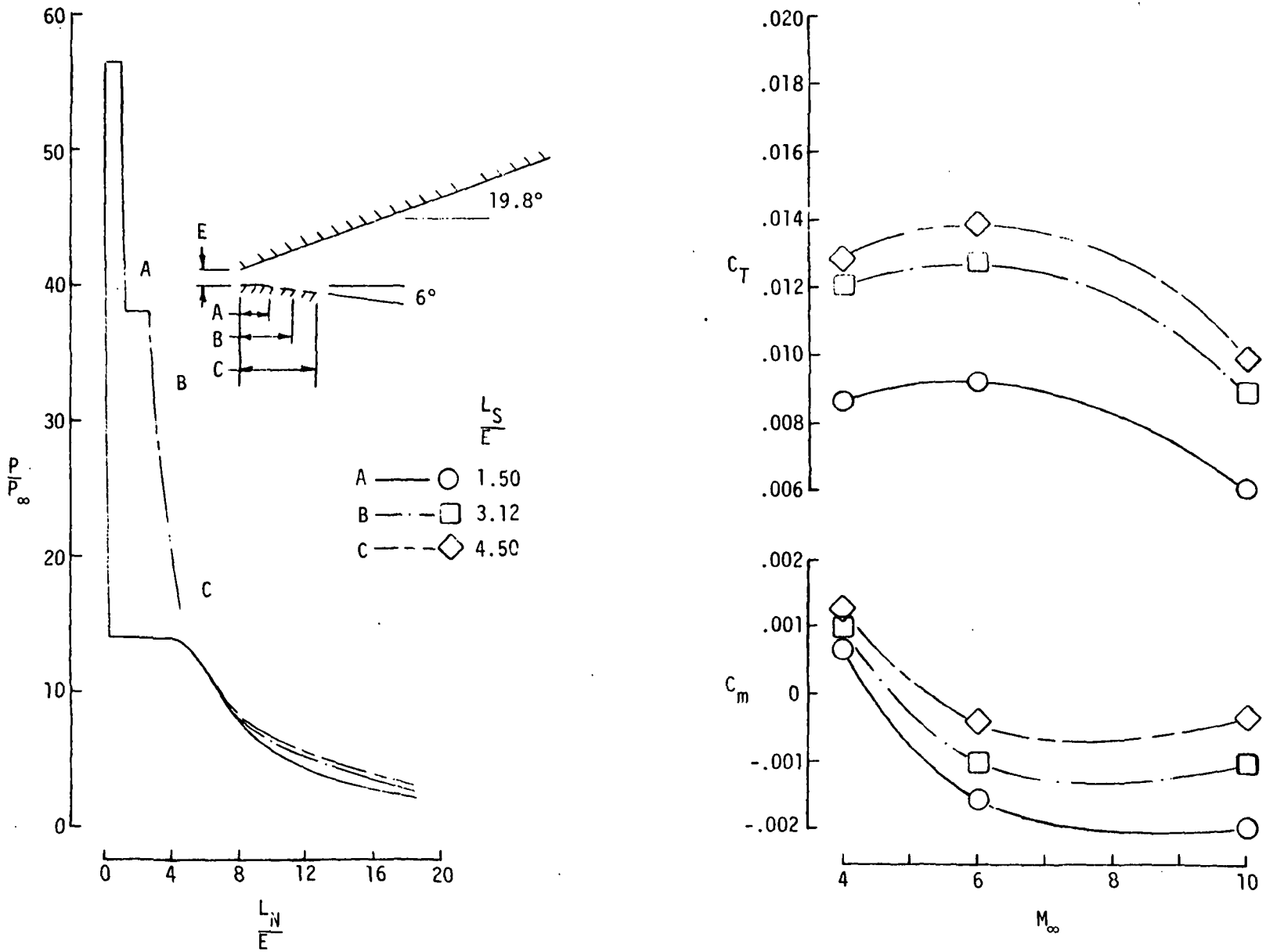

(a) NOZZLE PRESSURE DISTRIBUTIONS AT M_∞ = 10.

(b) NOZZLE THRUST AND MOMENTS

Figure 19.- Nozzle cowl length variation, q = 71850 n/m^2 (1500 psf), α = 2°.

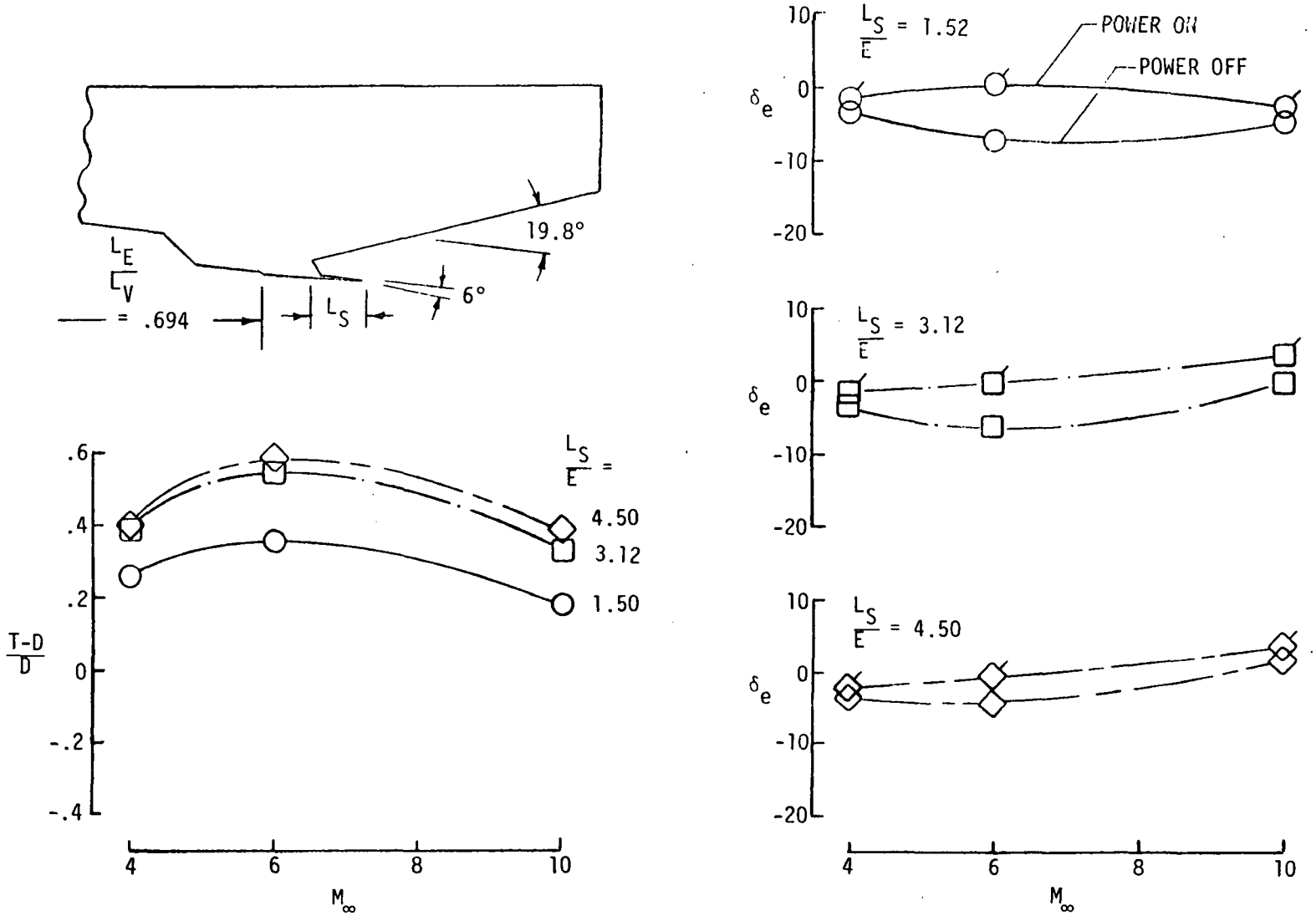

Figure 20.- Nozzle cowl length variation, q = 71850 n/m^2 (1500 psf), α = 2°.

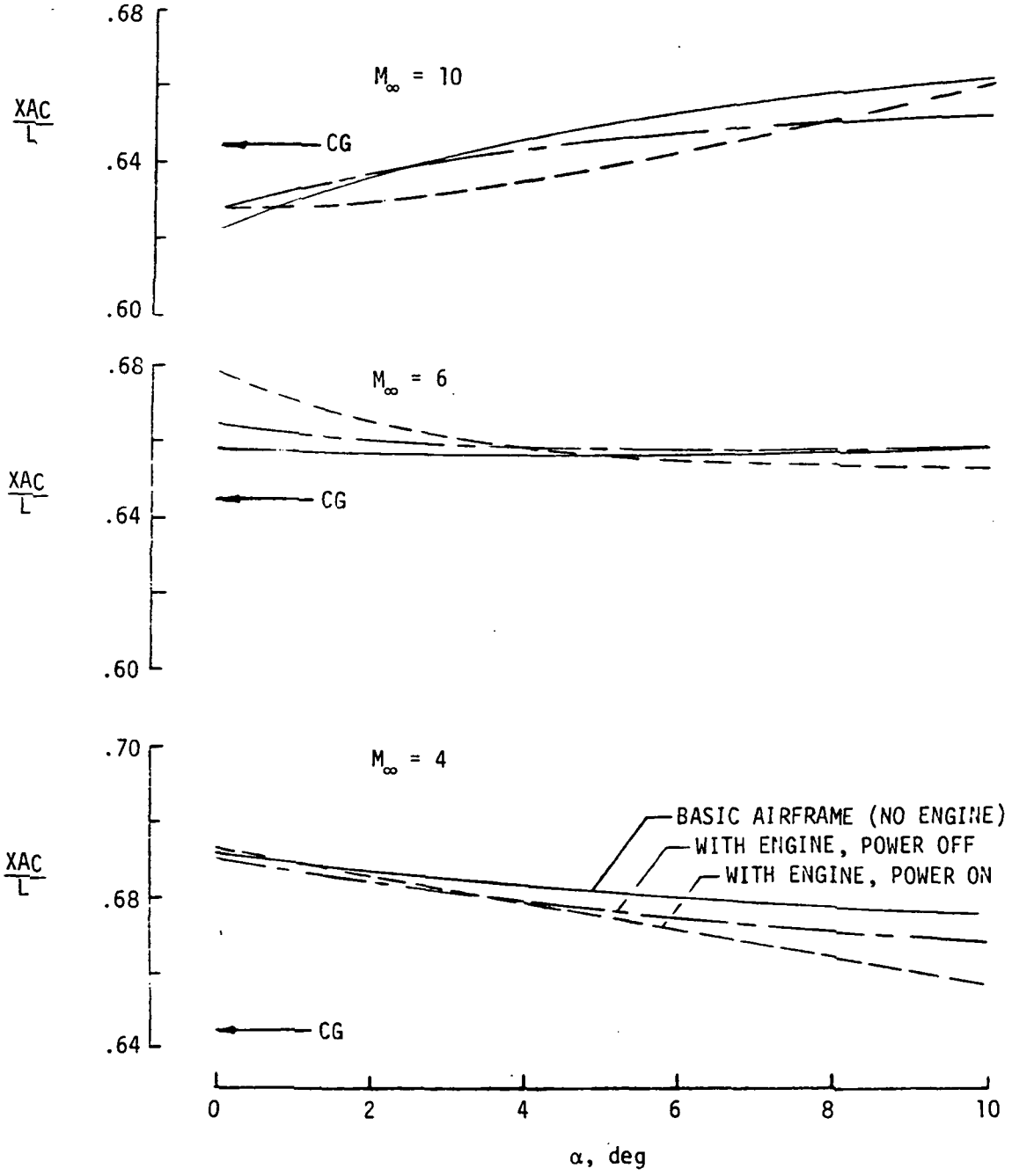

Figure 21.- Aerodynamic center location,
Vehicle CG = .645L, trimmed elevon setting.

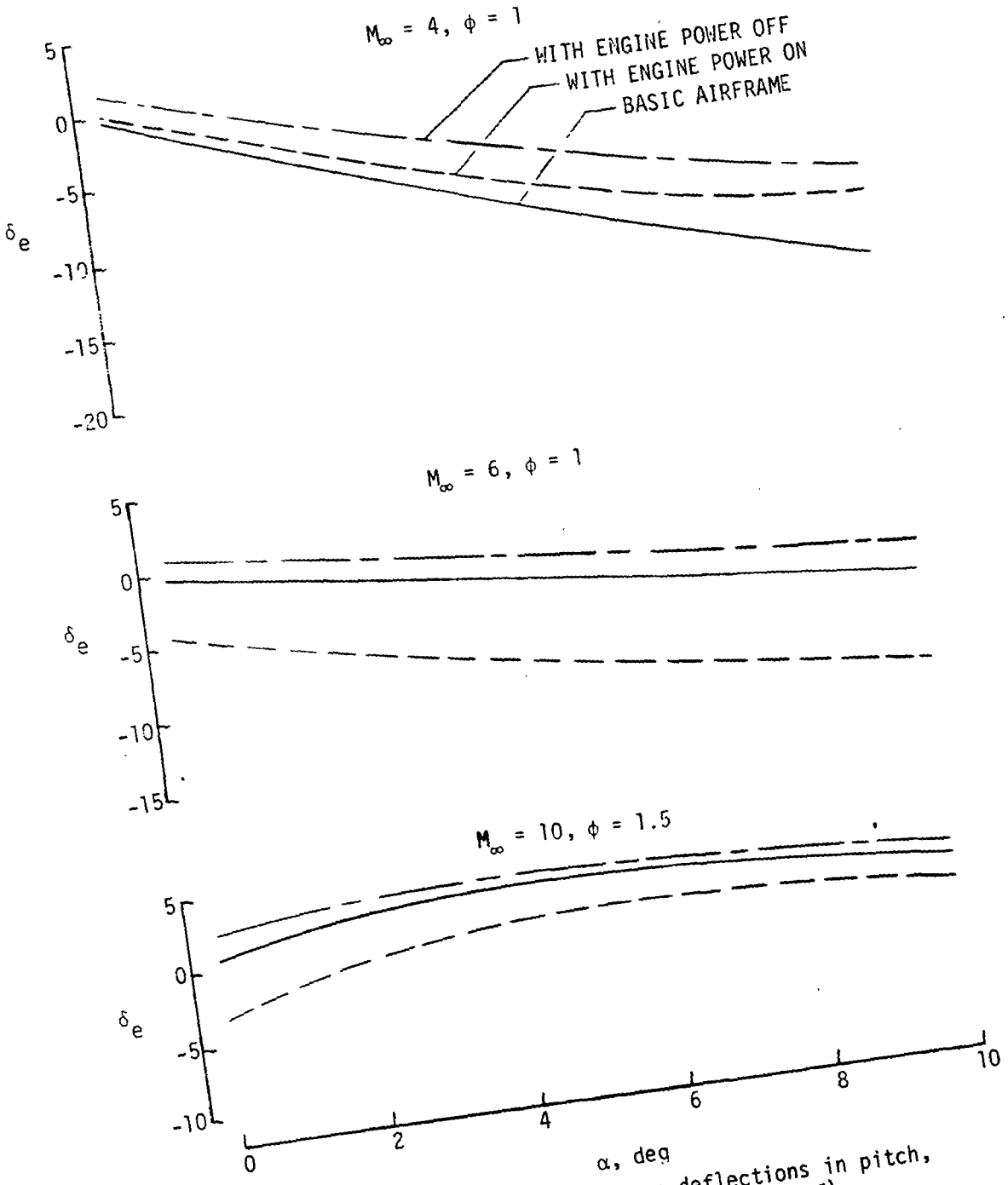

Figure 22.- Trim elevon deflections in pitch, $q = 71850$ n/m^2 (1500 psf).

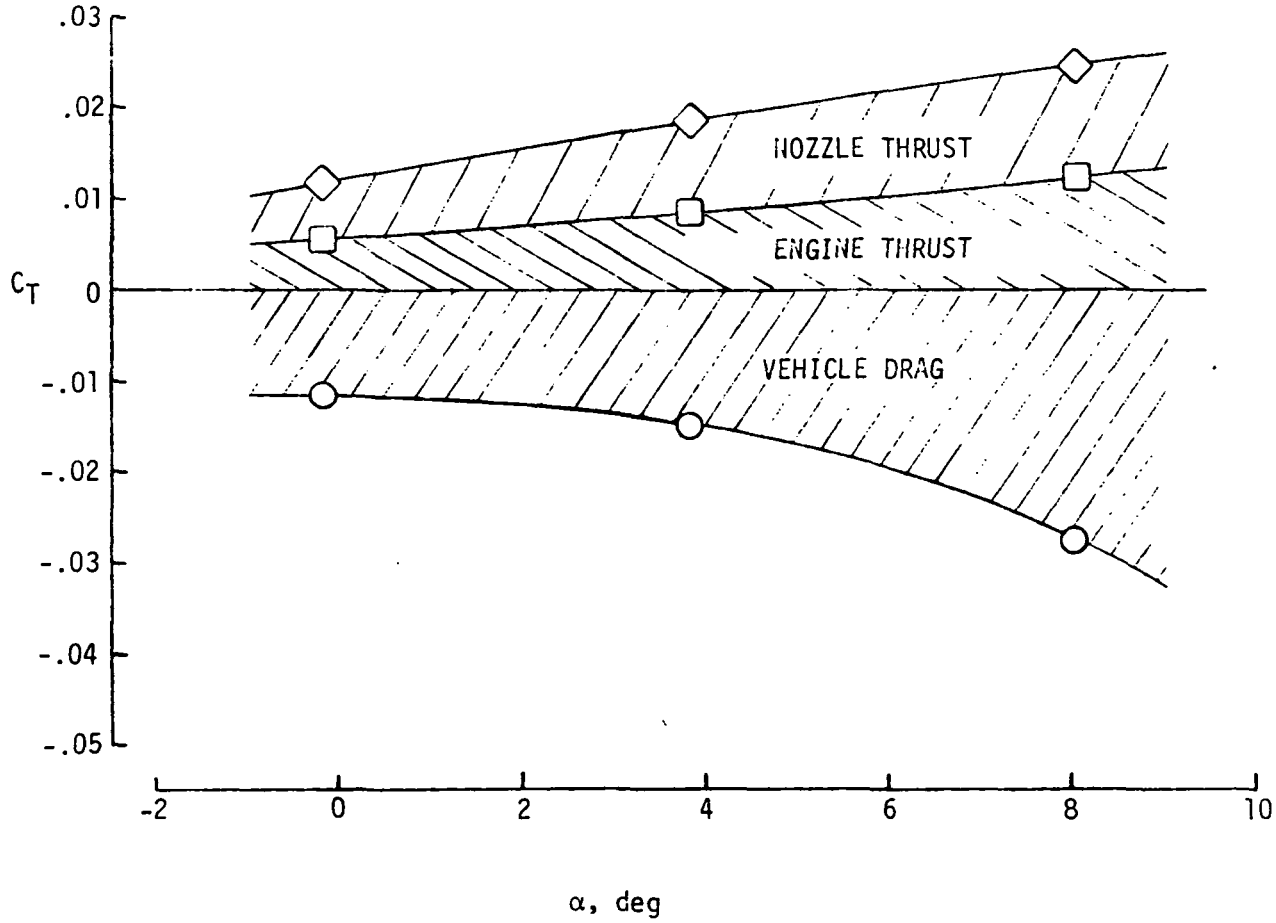

Figure 23.- Force components in flight direction, M_∞ = 10, q = 71850 n/m^2 (1500 psf).

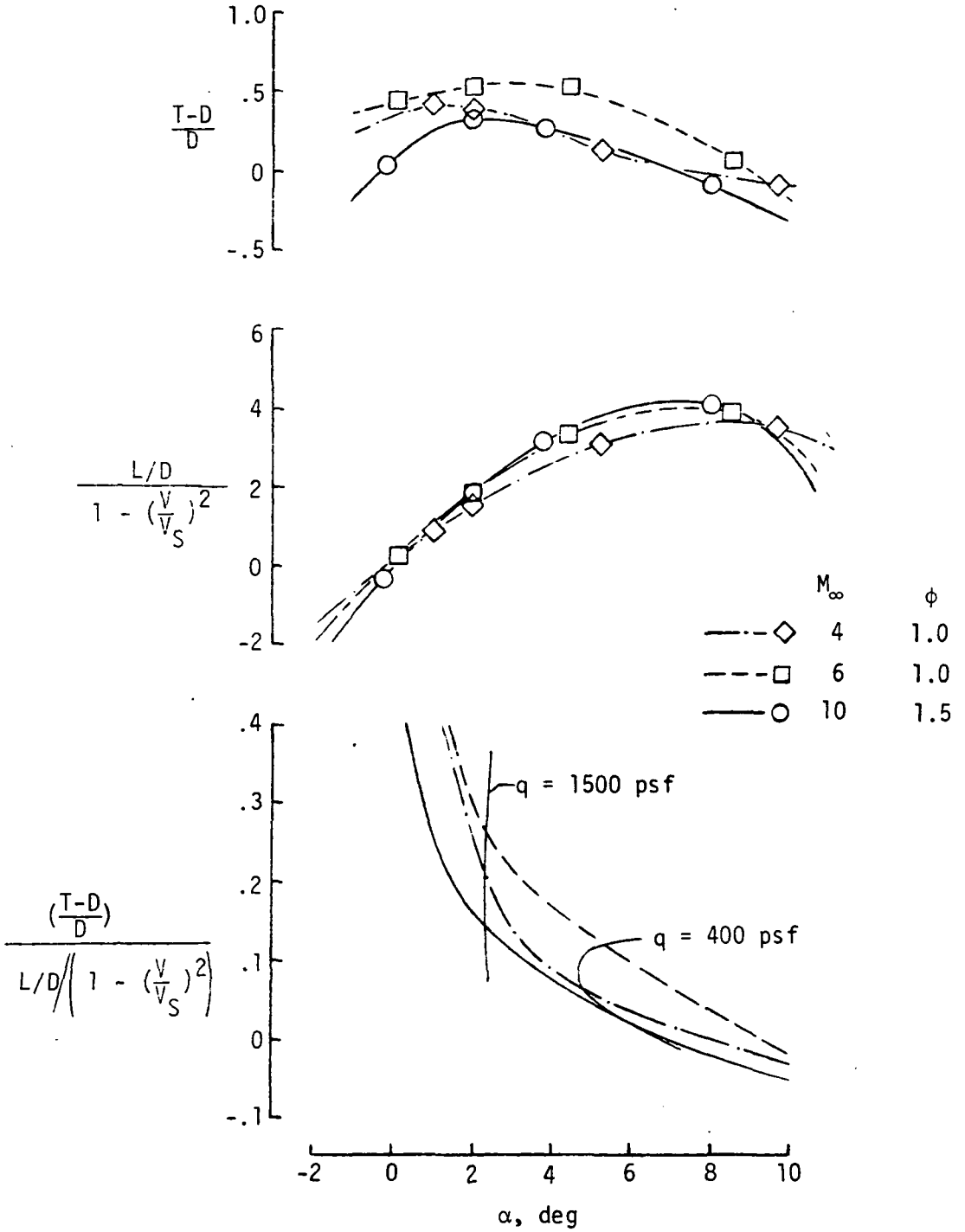

Figure 24.- Acceleration performance.